DYNAMIC SIMULATION OF THE TURBINE OF 110 MW UNIT OF PANKI THERMAL POWER STATION

by

PRADEEP K. SHAH

ME
1978
M
SHA
DYN

TH
ME 1978/M
Sh 13d

DEPARTMENT OF MECHANICAL ENGINEERING
INDIAN INSTITUTE OF TECHNOLOGY KANPUR

AUGUST, 1978

DYNAMIC SIMULATION OF THE TURBINE OF 110 MW UNIT OF PANKI THERMAL POWER STATION

A Thesis Submitted
In Partial Fulfilment of the Requirements
for the Degree of
MASTER OF TECHNOLOGY

by

PRADEEP K. SHAH

19[illegible]

to the

DEPARTMENT OF MECHANICAL ENGINEERING
INDIAN INSTITUTE OF TECHNOLOGY KANPUR

AUGUST, 1978

ME-1978-M-SHA-DYN

I.I.T. KANPUR
CENTRAL LIBRARY
Acc. No. A 55421

13 OCT 1978

23.8.78

CERTIFICATE

This is to certify that the work entitled "DYNAMIC SIMULATION OF TURBINE OF 110 MW UNIT OF PANKI THERMAL POWER STATION" by Shri Pradeep K. Shah has been carried out under our supervision and has not been submitted elsewhere for the award of a degree.

R. SINGH

P. V. GIRIJASHANKAR

Assistant Professors
Department of Mechanical Engineering
Indian Institute of Technology
Kanpur

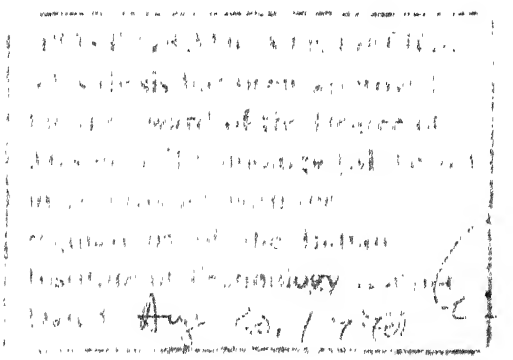

SYNOPSIS

A non linear mathematical model for the turbine of the 110 MW unit of Panki Thermal Power Station is developed. The model for the unit consisting of the high pressure, medium pressure and low pressure turbines, the reheaters, the condenser and the high pressure and low pressure feed water heaters, is simulated on a digital computer and open loop responses for a 10 MW load drop and step change in heat input to the reheaters have been obtained. Various results are discussed. Plant test conducted for a 10 MW load drop is compared with the model but extensive comparison of model responses with plant tests could not be made because of the lack of proper instrumentation available in the unit. A review of literature has been done and recommendations for further work are given.

ACKNOWLEDGEMENT

The author expresses his sincere gratitude to Drs. P.V. Girijashankar and R. Singh for suggesting the problem and their guidance throughout the period of this study.

The author is thankful to the Panki Thermal Power Station authorities for making the plant data available and for allowing to conduct some tests in the plant. In this connection special thanks are due to Mr. K.N. Srivastava, Mr. K.P. Aggarwal and Mr. Dhatia for taking deep interest in conducting the tests.

The author wishes to thank Dr. M.A. Pai for his keen interest in this problem and for his help in arranging plant tests.

The author also wishes to thank Dr. B. Sahay for many fruitful discussions that he had with him.

The author would like to thank many friends in Panki Power Station for their help. The author is particularly indebted to Messrs. Bhaskaran, Upreti and Mehta of Instruments Limited, Kota for many fruitful discussions and hospitality they offered during visits to the Panki Power Station. Thanks are due to Mr. Ramlu of BHEL for discussions and for making key data available. Further the author acknowledges the great help rendered by

Mr. Vishwakarma and Mr. Malhotra of Design Office, Panki Power Station in collecting the plant details.

Thanks are due to Mr. J.D. Verma for his patient and excellent typing and Mr. S.K. Misra for his patience and diligence in preparing the tracings.

Last but not the least author will like to thank his many friends who spent their invaluable time in helping him and without whose cooperation this work would not have been possible.

CONTENTS

LIST OF FIGURES

NOMENCLATURE

A_T	Normalised Flow area available for a partially opened valve
A_1, A_2	Equivalent areas for first and second reheater tubes respectively (m^2).
C_T, C, C_1, C_2, C_3	Constants used in flow, pressure relations for governing stage.
C_4, C_5, C_6, C_7, C_8	Constants used in the differential equations for flow.
C_{TM1}, C_{TM2}	Specific heat of the metal in reheater first and second respectively.
C_{RMS1}, C_{RMS2}	Constant used in determining the heat flow to steam in first and second reheater respectively.
C_{cw}	Constant used in the heat flux equation in the condenser.
C_{HMW1}, C_{HMW2}, C_{HMW3}, C_{HMW4}	Constants used in the heat flux equations in the four L.P. feed heater respectively.
C_{HMW5}, C_{HMW6}	Constants used in the heat flux equation in the two H.P. feedwater heaters respectively.
F_{R1}, F_{R2}	Friction factors for the Triflex and Exit reheater respectively.
H_{SS}	Enthalpy of steam before the throttle valves (Kcal/Kg).

H_{HP}	Enthalpy of steam at the exit of governing stage (Kcal/Kg)
H_{CR}, H_{CRA}	Ideal and actual cold reheat enthalpy of steam (Kcal/Kg)
H_{RO1}, H_{RO2} Exit	Enthalpy of steam at the exit of Triflex & reheater respectively (Kcal/Kg)
H_{ATMP}	Enthalpy of water used for attemperation (Kcal/Kg)
H_{MP1}, H_{MP2}, H_{MP3}, H_{MPO}	Ideal enthalpy of steam at the exit of each medium pressure (M.P.) turbine (Kcal/Kg)
H_{Mp1A}, H_{MP2A}, H_{MP2A}, H_{MPOA}	Actual enthalpy of steam at the exit of each medium pressure turbine (Kcal/Kg)
H_{LPO}, H_{LPOA}	Ideal and actual enthalpy at the exit of low pressure (L.P) turbine (Kcal/Kg)
H_{LH10}, H_{LH20}, H_{LH30}, H_{LH40}	Enthalpy of water at the exit of first, second, third and fourth low pressure feed water heaters respectively (Kcal/Kg)
H_{HH10}, H_{HH20}	Enthalpy of water at the exit of first and second high pressure feed water heater respectively (Kcal/Kg).
K_1	Constant used in the pressure, flow equation for the H.P. turbine

K_2, K_3, K_4, K_5	Constants used in flow pressure relations of the M.P. turbine
L_1, L_2	Equivalent length of tubes in the Triflex and Exit heater respectively (m)
M_{R1}, M_{R2}	Effective steam mass in reheater one and two respectively (Kg)
M_1, M_2	Metal mass of the reheater tubes (Kg)
P_{SS}	Steam pressure before the throttle valves (Kg/cm^2)
P_{THI} (I=1,2,3)	Nozzle ring pressure in the three streams (Kg/cm^2)
P_{HP}	Steam pressure at the exit of the curtis stage (Kg/cm^2)
P_{CR}	Cold reheat steam pressure (Kg/cm^2)
P_{RO1}, P_{RO2}	Steam pressure at the exit of Triflex and Exit reheater respectively (Kg/cm^2)
P_{MPI}	Inlet steam pressure to the medium pressure turbine (Kg/cm^2)
P_{MP1}, P_{MP2}, P_{MP3}, P_{MPO}	Steam pressure at the exit of each medium pressure turbine (Kg/cm^2)
P_{LPO}	Condenser pressure (Kg/cm^2)
POW_1	Power produced by the high pressure turbine (MW)
POW_2, POW_3, POW_4, POW_5	Power produced by each of the medium pressure turbine respectively (MW)

POW_6	Power produced by the low pressure turbine (MW)
Q_{RG1}, Q_{RG2}	Heat flux to the Triflex and Exit reheater metal walls respectively (Kcal/Sec.)
Q_{RS1}, Q_{RS2}	Heat added to the steam in the Triflex and Exit reheater respectively (Kcal/Sec.)
Q_{MW}	Heat given by the metal tubes to the condenser cooling water (Kcal/Sec.)
Q_{LH1MW}, Q_{LH2MW}, Q_{LH3MW}, Q_{LH4MW}	Heat added to the feedwater in the low pressure feed heaters number one, two, three and four respectively (Kcal/Sec.)
Q_{HH1MW}, Q_{HH2MW}	Heat added to the feed water in the two high pressure heaters respectively (Kcal/Sec.)
T_o	Time constant of the HP turbine (Sec.)
T_2, T_3, T_4, T_5	Time constants for the four medium pressure turbines (sec.)
T_6	Time constant of the low pressure turbine (Sec.)
T_7	Time constant of the Triflex reheater (Sec.)
T_8	Time constant of the Exit reheater (sec.)
T_{SS}	Steam temperature before the throttle valve (^oK)
T_{HP}	Temperature of steam at the exit of Curtis stage (^oC)
T_{CR}	Temperature of cold reheat steam (^oC)

T_{RM1}, T_{RM2}	Tube metal temperature in the Triflex and Exit reheater respectively (^{o}C)
T_{RS1}, T_{RS2}	Temperature of steam in the Triflex and Exit reheater respectively (^{o}C)
T_{MPI}	Temperature of steam at the inlet to medium pressure turbine (^{o}C)
T_{MP1}, T_{MP2}, T_{MP3}, T_{MPO}	Temperature of steam at the exit of the four medium pressure turbines respectively (^{o}K)
T_{LPO}	Temperature of steam in the condenser (^{o}C)
T_{CM}, T_{CW}	Temperature of tube metal and cooling water respectively in the condenser (^{o}C)
T_{HM1}, T_{HM2}, T_{HM3}, T_{HM4}	Tube metal temperature of the low pressure feed water heaters number one, two, three and four respectively
T_{HM5}, T_{HM6}	Tube metal temperature of the two high pressure feed water heaters respectively (^{o}C)
T_{HW1}, T_{HW2}, T_{HW3}, T_{HW4}	Temperature of feed water in the four low pressure feed heaters respectively (^{o}C)
T_{HW5}, T_{HW6}	Temperature of feed water in the two high pressure feed water heaters respectively (^{o}C)
V_{R1}, V_{R2}	Effective steam volume in reheaters Triflex and Exit respectively (m^3)

W_T	Total steam flow at a particular load (Kg/Sec.)
$(W_T)_V$	Flow through the throttle valve (Kg/sec.)
$(W_T)_N$	Flow through the nozzle ring (Kg/Sec.)
W_{CR}	Cold reheat steam flow (Kg/Sec.)
W_R	Rated flow of the turbine (Kg/Sec.)
W_N	No load flow of the turbine (Kg/Sec.)
W_L	Ratio of W_N and W_R ($W_L = W_N/W_R$)
W_{RI2}	Steam flow at the inlet of the Exit reheater (Kg/Sec.)
W_{RO1}, W_{RO2}	Steam flow at the exit of Triflex and Exit reheater respectively (Kg/Sec.)
W_{ATMP}	Attemperation flow added to the steam before the M.P. turbine inlet (Kg/sec.)
W_{MPI}	Steam flow entering the medium pressure turbine (Kg/Sec.)
W_{MP1}, W_{MP2}, W_{MP3}, W_{MPO}	Steam flow at the exit of the four medium pressure turbines respectively (Kg/Sec.)
W_{LPO}	Flow to the condenser (Kg/Sec.)
W_{CW}	Quantity of cooling water in the condenser (Kg/Sec.)
W_{LM1}, W_{LH2}, W_{LH3}, W_{LH4}	Quantity of feed water passing through the four low pressure feed water heaters respectively (Kg/Sec.)
W_{HH1}, W_{HH2}	Quantity of feed water passing through the high pressure feed water heaters respectively.

ρ_{SS}	Density of steam before the throttle valve (Kg/m^3)
ρ_{THI}	Density of steam in the nozzle ring (Kg/m^3)
ρ_{HP}	Density of steam at the exit of governing stage (Kg/m^3)
ρ_{R1}	Density of steam in the Triflex reheater (Kg/m^3)
ρ_{R2}	Density of steam in the Exit reheater (Kg/m^3)
ρ_{MP1}	Density of steam at the exit of first M.P. turbine (Kg/m^3)
ρ_{MP2}	Density of steam at the exit of second M.P. turbine (Kg/m^3)
ρ_{MP3}	Density of steam at the exit of third M.P. turbine (Kg/m^3)
η_{HP}, η_{MP}, η_{LP}	Thermodynamic efficiencies of the high pressure, medium pressure and low pressure turbines respectively.
η_F	Efficiency corrections factor for the high pressure turbine.
η_{F1}, η_{F2}, η_{F3}, η_{F4}	Efficiency correction factor for each of the four M.P. Turbines
η_{F5}	Efficiency correction factor for L.P. Turbine

η_{HPA}	Actual efficiency of the H.P. turbine
η_{MP1}, η_{MP2}, η_{MP3}, η_{MP4}	Actual efficiencies of each of the four M.P. turbines
η_{LPA}	Actual efficiency of the low pressure turbine

CHAPTER 1

INTRODUCTION

Economic prosperity and social progress of a developing country like ours is heavily dependent on how we utilize our power generation resources. There are three major sources of energy viz. Hydro power, Thermal power and Nuclear power. The hydro power potential of our country is large but it is restricted by factors like large initial investment, long gestation period, excessive dependence on monsoon etc. Nuclear power generation prospects are not very bright due to economic, political and technological considerations. As a result, the current trend is to go for more and more fossil fuel fired plants. Of the existing generation capacity of 26,000 MW, the hydel sources account for 40 percent. The next five years plan projection envisages augmentation of installed capacity by 18,500 MW. Of this 13,000 MW will come from coal fired thermal stations, 3,800 is assigned to hydel and the balance to Nuclear plants. So bulk of the power will come from thermal and super thermal power stations.

A modern power station is a gigantic complex by itself and consists of several sub-systems and innumerable components. The performance of the overall plant

depends critically upon the functioning of these components and sub-systems. Besides, demand for higher efficiency is leading towards higher steam pressures and temperatures. There is also a tendency to go in for larger and larger unit sizes for reduction of capital costs. On the other hand, more and more stringent requirements are imposed regarding safety and control. All these have led to the development of modern power systems and power stations with highly complex instrumentation and control systems, quite often aided by computers for on line data logging, monitoring and in a few cases for control purposes.

It is in this context that understanding of the power plant dynamics becomes important. Smooth functioning of the plant depends upon the nature of the interaction between the various subsystems. How well a plant behaves, is determined not only by its steady state performance, but to a large extent by how it reacts to disturbances and abnormal conditions. These disturbance consist of momentary or long time malfunctioning of internal components or external disturbances. Plant control and safety system must override such situations and outages. Effective steps can only be taken if behaviour of the system is fully understood and only then can suitable control and safety systems be engineered to meet the situation.

Dynamic simulation in such conditions becomes a very important tool because of following reasons:

1. It is not feasible to create major power system disturbances for the purpose of examining system behaviour and effectiveness of proposed strategies or actions. Experimental evaluation of strategies is therefore impractical. Simulation can be used to judge the merits of these strategies under such major disturbances. Moreover sensitivity of these strategies to system changes and system model parameters can also be determined.

2. By developing models for different components much insight is gained into the unit dynamic characteristics, control potential and system behaviour.

3. Simulation provides a means of evaluating the system behaviour and helps in predetermining the critical parameters and their response to operator action etc.

4. Power system dynamics (upto several minutes following a major system upset) are not well understood and simulation helps in this regard.

Generally three kinds of problems are studied in dynamic analysis of power systems. First, the study of instability that may occur when there is a fault on

the generator side. This kind of study is done over few seconds of the plant operation. Second, the study of the response of the system to load changes. This study is done over few minutes. Third, the study of start up and shut down etc. which are carried over for few hours.

It is the second category in which the present problem falls. The first step towards conducting such a study is developing a mathematical model which adequately describes the system behaviour over the interval needed for that particular problem. This requires a thorough understanding of the component systems, and processes and their interaction.

As the features of a particular unit differ from one power plant to another, need was felt for developing a model for a unit which is most representative of the current boiler turbine units being used in our country. Proximity to I.I.T. Kanpur weighed heavily in selecting the 110 MW unit of Panki Thermal Power Station for this purpose. The model for the boiler unit of the plant was developed earlier [1]. In the present study an attempt is made to model the plant following the steam path downstream of superheater and back to drum through the regenerative feed heaters. The plant was also made available for open loop tests by the kind cooperation of the plant management.

1.1 LITERATURE REVIEW

Investigations in the power station modelling started in late fifties when many investigators considered the problem of drum type boiler modelling. In 1958 Chien et al. [2] first presented a model and the dynamic analysis for a drum type boiler. The plant considered was an oil fired, single furnace natural circulation unit. The model consisting of a set of differential equations was solved using electronic differential analyser and a few open loop responses were obtained. But the model was too simple to represent the complicated dynamics of the boiler.

Daniels et al. [3] in 1960 developed a model for the 200 MW unit of the Philadelphia Electric Co., Crombay which was a pulverised coal fired, twin furnace, controlled circulation, reheat boiler. Extensive open loop tests were carried out in the actual plant in order to validate the model. But the model did not produce sufficiently accurate responses to be considered suitable for control system design.

In 1965, Thompson [4] derived a linearised mathematical model describing the dynamics of the drum, downcomer, waterwall, economiser, superheater and combustion subsystems of a large utility power plant. Sufficiently accurate transient responses were obtained to permit the

performance evaluation of proposed multivariable controllers. The model was verified by transient tests on the Crombay unit of Philadelphia Electric Co. But this model was not developed for the full plant and was terminated at the throttle valve. Moreover, because of large number of elemental volumes, the model had a large state space dimension rendering it unsuitable for extensive control system analysis.

IBM report [6] also presented a model for most general type of boiler and turbine using lumped parameter technique. Open and closed loop responses of the system were obtained and analog closed loop control operation was incorporated in the simulation model. Controller settings are determined using Ziegler - Nichols techniques based on single loop responses.

In 1970, Mcdonald et al. [7,8,9] developed an extensive nonlinear mathematical model of a drum type, twin furnace, reheat, boiler-turbine-generator system. The results of an extensive programme of comparisions of closed loop steady state operation and open loop transient responses of field data and the model are reported to substantiate the validity of the model. The relatively low order of the model, its high degree of accuracy in representing the relevant responses and its development

on the basis of a first principle analysis, make it ideal for control system analysis and design. The model parameters are physical quantities which are readily obtainable from design data or unit acceptance test data. The model can be adapted to other applications also.

In the present model the multivalve approach followed by Mcdonald et al. [9] for the governing stage modelling is adopted. In the existing literature for the turbine modelling the medium pressure and low pressure turbines are lumped together and extractions are assumed to be taken at the end of the turbine. But, in the present model the medium pressure (MP) and low pressure (LP) turbines are modelled seperately. Moreover, the MP turbine is subdivided into four smaller turbines to account for the reduced steam flow in the succeeding stages after each extraction. Furthermore, all the feedwater heaters are considered seperately instead of lumping them into one feedwater heater as has been done upto now by other researchers. A brief outline of the content of each chapter is given below.

In Chapter 2 plant description has been given. Flow path taken by main steam, condensate water and feed water has been presented and explained in detail.

In Chapter 3 the complete mathematical model of the plant has been developed. Further, assumptions and simplifications made in the process of developing the model have also been listed.

In Chapter 4 the results have been discussed. Plant responses have been obtained for a 10 MW load drop and responses to some variables have been compared with the results obtained from plant tests. Also steady state data from the plant has been compared with the steady state data of the model. This chapter is concluded with a list of topics for research for further work.

CHAPTER 2

PLANT DESCRIPTION

The Panki Thermal Power Station comprises of two old units of 32 MW each to which two new units of 110 MW each have been added recently. The second unit of 110 MW known as Unit No. 2 of the Panki Thermal Station Project is manufactured by the Bharat Heavy Electricals Limited, India and was selected for modelling purposes.

The unit consisting of a boiler and turbine is a single drum type, reheat, closed cycle system with regenerative feed heating. The boiler is a single drum, radiant water tube, dry bottom circulation, pulverised coal fired one with superheater and reheater. Since our study pertains to only the turbine part, the detailed specifications are listed in Appendix 1 and the plant details are shown in Figure 1.

The flow of steam from the secondary superheater bifurcates into two equal halves and each half, after passing through a normally open throttle valve, enters a steam chest on either side of the turbine. Each steam chest contains four governing valves that are opened sequentially to control the flow of steam to the turbine as shown in Figure 2. Each valve discharges the steam

to its own section of the first stage nozzle ring. The valves are regulated by secondary oil pressure which can be remotely controlled by a pump. This pump is driven by an electrical motor and can be controlled from the control room. Valves 1 and 2 open at the same secondary oil pressure. The different pressures at which these valvesopen and are fully open are given in Appendix 1. Two nozzle ring sections contain seven nozzles each and the other two eight nozzles each. The steam leaving the governing valve is expanded through these convergent divergent nozzles and emerges at high velocity to impinge upon two rows of moving blades called the 'Curtis Stage' or the 'governing stage'. This is followed by eight impulse stages of the high pressure turbine at the exit of which some steam is extracted for the high pressure feed water heater No. 2. The bulk of the exit steam from the H.P. turbine passes through a series of two reheaters called Trifflex and Exit reheater respectively. Exit reheater is in the first pass of the boiler and the Triflex in the second pass of the flue gases (not shown in figure). Steam from exit reheater with temperature controlled at 535 ^{o}C by attemperation is fed into the Medium Pressure Turbine which consists of twelve impulse stages. Steam is extracted at the end of 4th, 8th, 10th and 12th stages and is fed to High Pressure Feedwater Heater 1, Deaerator, Low Pressure Heater 5 and Low Pressure Heater No. 4 respectively in

that sequence. Steam from the exit of medium pressure turbine is fed directly into a double-flow low pressure turbine which consists of four reaction stages on each side. Steam is extracted from both the sides at the end of 1st, 2nd and 3rd stages and is fed into the low pressure feed-water heater 3, low pressure heater 2 and low pressure heater 1 respectively. The steam exiting from the low pressure turbine is condensed in two condensers each, and the condensate is passed through the series of low pressure feed heaters mentioned above. The steam condensed in the LP heaters 1 and 2 is fed back to main line before the feed water enters LP heater 1. Condensate from LP heaters 3, 4 and 5 is fed into main flow line at the entrance of the LP heater 3. From the exit of the LP heater 5 the feed water is taken to the 'Feed Water Tank' through the deae-rator. From the feed water tank, water is taken to the two high pressure heaters with the help of a feed water pump. The steam condensed in the two heaters is fed back into the main line at the entrance of high pressure heater 1. Exiting water from these heaters goes to the economiser where it is heated by the flue gases and is then passed on to the boiler drum. The details of flow path and other details from here onwards can be found in Reference [1].

CHAPTER 3

MATHEMATICAL MODELLING

3.1 GENERAL COMMENTS

Panki Thermal Power Station details are given in three drawings [15]. These being erection drawings they describe the plant in great details which is not required for the present study. Hence, Figure 1 shows a simplified version of the turbine unit, the main steam path, feed water and condensate water lines which was obtained from the above three referred drawings. Even this diagram was too detailed because it included some features which will become operational only in case of emergencies or turbine trips. Hence it was further simplified and Figure 3 shows the plant diagram as it was modelled. Steam admission to the high pressure turbine is controlled by four valves which admit steam to a nozzle ring followed by two rows of moving blades with an intervening row of fixed guide blades. These constitute the governing stage of the turbine. The governing stage is followed by eight impulse stages of the H.P. Turbine. After the H.P. Turbine some steam (approximately 8%) is extracted for passing it through high pressure feed water heater No. 1 and the rest is passed through two reheaters called Triflex reheater and the Exit reheater as discussed in Chapter 2.

To obtain good representation for dynamic studies, the medium pressure turbine is subdivided into four smaller turbines with the lumping made at the end of each extraction. This results in first and second turbines having four stages each while third and fourth have two stages each. The extraction steam, from various extraction points in the M.P. Turbine, is taken to high pressure feed water heater No. 2, the feed water tank and low pressure feed water heaters No. 5 and 4 respectively in that order. Outlet steam from the medium pressure turbine is fed into low pressure turbine. The arrangement of this turbine is symmetric and as such, is replaced with a simple four stage turbine using the principle of symmetry. The steam that is being extracted at 3 points in the LP turbine is assumed to be extracted at the exit of each turbine section and is utilised for heating the feed water in heater Nos. 3, 2, and 1 respectively. The two condensers, one each for the two sides of the low pressure turbine are also lumped into one. The condensate then passes through two low pressure feed water heaters which have been lumped into one as shown in Figure 3 . The bypass line to condensate storage tank is used only in emergency conditions and has not been modelled. The feed water then passes through feed water heater Nos. 2, 3 and 4 and then is fed into feed water tank. From this tank feed water is pumped into the high

pressure feed water heater No. 1 and then to the No. 2 heater. From there the feed water goes to boiler drum through the economiser.

In developing the model, the system approach has been followed and the components are considered to be blocks across which the physical changes in the condition of steam or water, as the case may be, are considered. These changes are represented in the form of mathematical equations by applying mass balance, momentum balance and energy balance across these blocks. The thermodynamic path of the process as it flows through the turbine is given in Figure 9. The details of the model are presented below.

3.2 GOVERNING STAGE MODELLING

There are four throttle valves to control the admission of steam to the high pressure turbine. The lift of these valves is controlled by the oil pressure. Out of these four valves, two throttle valves attain fully open position at the same oil pressure and hence these two have been lumped into one. As a result the steam admission has been modelled to take place through three valves which open sequentially as the load is increased. Following assumptions are also made:

1. steam condition at the inlet of the valve is same for all the three streams,
2. steam flows in three streams caused by the three valves and undergoes different changes in steam condition, however pressure at the exit of governing stage is same for all the three streams,
3. impulse blades ideally absorb all kinematic energy in the incoming steam and converts it into work.

With the above assumptions, mass flow rate through the throttle valve is related to the pressure drop across it by the following equation [9]

$$(W_T)_V^2 = \frac{A_T^2}{C_T} \rho_{SS} (P_{SS} - P_{THI}) \qquad (3.1)$$

where

$(W_T)_V$ = flow through the throttle valve (Kg/sec.),

A_T = flow area available for a partially open valve (Normalised),

ρ_{SS} = density of steam at the valve inlet (Kg/m^3),

P_{SS} = steam pressure at the valve inlet (Kg/cm^2),

P_{THI} = nozzle ring pressure in three streams respectively (Kg/cm^2),

C_T = a constant.

Mass flow rate through the nozzle ring is given by

$$(W_T)_N^2 = C \rho_{THI} (P_{THI} - P_{HP}) \qquad (3.2)$$

where,

$(W_T)_N$ = flow through the nozzle ring (Kg/sec.),

C = a constant,

ρ_{THI} = density of steam in the nozzle ring (Kg/m^3),

P_{HP} = steam pressure at the exit of curtis stage (Kg/cm^2).

Assuming no storage in the nozzle ring the flows given by Eqns. 3.1 and 3.2 are equal, so we get the following equation for flow

$$(W_T)^2 = C_1 \rho_{SS} (P_{SS} - P_{HP}) \qquad (3.3)$$

Here

$$C_1 = \frac{A_T^2 C \rho_{THI}}{(A_T^2 \rho_{SS} + C_T \rho_{THI} C)}$$

and W_T = total steam flow at a particular load (Kg/sec.).

For a fully open valve $A_T = 1$ and flow is given by a similar equation

$$(W_T)^2 = C_2 \rho_{SS} (P_{SS} - P_{HP}) \qquad (3.4)$$

where

$$C_2 = \frac{C \rho_{THI}}{(\rho_{SS} + C_T \rho_{THI} C)}$$

If the pressure ratio across the valve nozzle combination is less than the critical (P_{HP}/P_{SS} < 0·5054) then sonic conditions exist and flow is independent of the down stream conditions. In such a case the flow through a partially open valve is given by [9]

$$W_T = A_T \; C_3 \; \frac{P_{SS}}{\sqrt{T_{SS}}} \qquad (3.5)$$

where,

T_{SS} = temperature of steam at valve inlet (^{o}K),

C_3 = a constant.

Flow through a fully open valve is given (similar to Eq. 3.5 with A_T = 1) by

$$W_T = C_3 \; \frac{P_{SS}}{\sqrt{T_{SS}}} \qquad (3.6)$$

Once the total flow through the turbine, (W_T) is known, the preceeding equations are used to determine the pressure at the exit of the governing stage. But the situation becomes complicated if critical pressure ratio exists across the nozzle (i.e. P_{THI}/P_{HP} < 0·5054 for super-heated steam). In such cases any one combination of the following i.e. fully open subsonic, fully open sonic, partially open subsonic and partially open sonic conditions may occur. A generalised program has been developed to

take into account all such situations. The flow chart for this is given in Fig. 4 . First oil pressure is determined from the known load value (Fig. 5) and a value of the governing stage exit pressure (P_{HP}) is assumed. The status of a particular valve i.e. whether it is partially open or fully open is determined with the help of this oil pressure (Fig. 6). Now the partially open stream flow is determined using Eqn. 3.3. For the fully open streams a check is made to determine whether critical pressure ratio ($P_{SS}/P_{HP} < 0.5454$) exists across the valve nozzle combination. If critical pressure ratio does not exist, the flow is determined using Eqn. 3.4 while if critical pressure ratio exists Eqn. 3.6 is used. At this stage the sum of the three stream flows determined above is computed and is compared with the total turbine flow (W_T). If the total of these individual flows is not equal to the total turbine flow (W_T), then the assumed P_{HP} value is modified and the individual flows are determined again using this modified value. This procedure is repeated and the program is terminated when we get the sum of three stream flows equal to the turbine flow within prescribed accuracy.

At this stage a check is made to see whether all valves are fully open. If the answer is yes, then the down stream pressure, temperature and enthalpy are determined using appropriate equations given below

(Eqns. 3.7 to 3.13). If all valves are not fully open, then a combination of partially open and fully open valves will exist. For the partially open valves the pressure P_{THI} in the nozzle ring is calculated using the subsonic flow equations 3.2. With this pressure known, the ratio P_{THI}/P_{HP} is calculated. This ratio then gives the number of sonic and subsonic partially open streams. Suppose subsonic flow exists in all the three streams then the above calculated P_{THI} and P_{HP} values are valid and the down stream pressure, temperature, enthalpy can be easily determined using Eqns. 3.7 to 3.15. If a combination of sonic and subsonic flow streams exists then the subsonic stream flow is calculated with the values of P_{THI} and P_{HP} determined above while for the sonic streams P_{THI} is determined by equating subsonic flow through the valve to sonic flow through its corresponding nozzle. Thus with this P_{THI} the flows through these sonic streams are also determined using Eqn. 3.2. The sum of these sonic and subsonic flow is now evaluated and compared with the total turbine flow (W_T). If these two flows are not equal, P_{HP} is again modified and the procedure is repeated until we get the sum of flows equal to the turbine flow within the desired accuracy. With the P_{HP} known the enthalpy and temperatures are determined using equations 3.7 to 3.15 described below.

Following are the state relations for determining nozzle ring steam temperatures obtained by using empirical fits from steam tables [16]

$$T_{TH1} = 0.5\ P_{TH1} + 1.33\ H_{TH1} - 620.0 \qquad (3.7)$$

where

T_{TH1} = first stream nozzle ring temperature (^{o}C)

H_{TH1} = first stream nozzle ring enthalpy (Kcal/Kg).

$$T_{TH2} = 0.5\ P_{TH2} + 1.33\ H_{TH2} - 620.0 \qquad (3.8)$$

where

T_{TH2} = second stream nozzle ring temperature (^{o}C),

H_{TH2} = second stream nozzle ring enthalpy (Kcal/Kg).

$$T_{TH3} = 0.5\ P_{TH3} + 1.33\ H_{TH3} - 620.0 \qquad (3.9)$$

where

T_{TH3} = third stream nozzle ring temperature (^{o}C),

H_{TH3} = third stream nozzle ring enthalpy (Kcal/Kg).

Ideal exit temperatures of steam in the nozzles are determined by using the isentropic laws given by the following expressions

$$T_{HP1} = T_{TH1} \left(\frac{P_{HP}}{P_{TH1}} \right)^{\frac{n-1}{n}} \qquad (3.10)$$

where

T_{HP1} = first stream nozzle ring exit temperature (^{o}C),

n = index for super heated steam (n = 1.3).

$$T_{HP2} = T_{TH2} \left(\frac{P_{HP}}{P_{TH2}} \right)^{\frac{n-1}{n}} \qquad (3.11)$$

where

T_{HP2} = second stream nozzle ring exit temperature (^{o}C),

$$T_{HP3} = T_{TH3} \left(\frac{P_{HP}}{P_{TH3}} \right)^{\frac{n-1}{n}} \qquad (3.12)$$

Nozzle ring exit enthalpy is determined using empirical fits obtained from steam tables for following state relations.

$$H_{HP1} = -0.3\, P_{HP} + 0.617\ T_{HP1} + 527.6 \qquad (3.13)$$

where

H_{HP1} = enthalpy of steam for first stream at nozzle ring exit (Kcal/Kg).

$$H_{HP2} = -0.3\, P_{HP} + 0.617\ T_{HP2} + 527.6 \qquad (3.14)$$

where

H_{HP2} = enthalpy of steam for second stream at nozzle exit. (Kcal/Kg).

$$H_{HP3} = -0.3\, P_{HP} + 0.617\ T_{HP3} + 527.6 \qquad (3.15)$$

where

H_{HP3} = enthalpy of steam for third stream at nozzle exit (Kcal/Kg).

The average enthalpy of the three streams is determined by taking a weighted average of the enthalpies of the three streams using the energy balance equation.

3.3 HIGH PRESSURE TURBINE MODELLING

Steam coming out of the governing stage enters the high pressure turbine. For modelling, it is assumed that high pressure turbine impulse blades ideally convert the kinetic energy into work. Further, it is assumed that the relationship between enthalpy, specific volume and pressure for the superheated steam follows Callender's empirical relationship for all non-constant pressure processes [6].

The flow through the high pressure turbine is related to the pressure drop across it by following equation [10]

$$(W_T)^2 = K_1 \rho_{HP} (P_{HP} - P_{CR}) \qquad (3.16)$$

where

K_1 = a constant to be determined at initialisation time,

P_{CR} = cold reheat steam pressure (Kg/cm^2).

The change in the outlet flow of turbine with a change in turbine inlet flow, as indicated by the following equation [6], is determined by considering the turbine to have a first order transfer function.

$$\frac{d(W_{CR})}{dt} = \frac{(1 - C_0)\, W_T - W_{CR}}{T_0} \qquad (3.17)$$

where

W_{CR} = steam flow at the turbine outlet (cold reheat flow)(Kg/Sec.),

C_0 = a constant,

T_0 = time constant for the high pressure turbine (Sec.).

Expansion of steam in the turbine is assumed to be isentropic ($n = 1.3$) and the isentropic temperature of the cold reheat steam is given by the following equation [10].

$$T_{CR'} = T_{HP} \left(\frac{P_{CR}}{P_{HP}} \right)^{\frac{n-1}{n}} \qquad (3.18)$$

where

T_{CR} = temperature of the cold reheat steam (^{o}K),

T_{HP} = temperature of steam at governing stage exit (^{o}K),

n = index for the superheated steam.

Value of n is taken to be 1.3 for superheated steam [10].

Following state relation is used to determine the ideal cold reheat enthalpy in terms of cold reheat pressures P_{CR} and cold reheat temperature, T_{CR}

$$H_{CR} = 0.5934 \; P_{CR} + 0.65 \; T_{CR} + 534.069 \qquad (3.19)$$

where

H_{CR} = cold reheat steam enthalpy (Kcal/Kg).

The overall efficiency of the turbine is reduced by the effects of stage leakages, root and tip interference losses and rotational losses which increase with the flow rate. These factors are grouped together in the model, in the form of a efficiency correction factor [6]

$$\eta_F = \frac{(\frac{W_{CR}}{W_R}) - W_L}{(\frac{W_{CR}}{W_R})\,(1 - W_L)} \qquad (3.20)$$

where

η_F = efficiency correction factor for the high pressure turbine,

W_R = rated steam flow of the turbine (Kg/Sec.),

W_L = ratio of no load flow to the rated flow of the turbine.

Variation of efficiency correction factor, with the ratio of actual turbine flow to the rated flow, is shown in Fig. 8.

The overall efficiency is given by

$$\eta_{HPA} = \eta_{HP} \eta_F \quad (3.21)$$

where

η_{HP} = thermodynamic efficiency.

The actual reheat enthalpy (Referring to Fig.9) is given by

$$H_{CRA} = H_{HP} - \eta_{HPA} (H_{HP} - H_{CR}) \quad (3.22)$$

where

H_{CRA} = actual cold reheat steam enthalpy (Kcal/Kg).

The power produced by the HP turbine in terms of the flow rate and enthalpy drop in the HP turbine is given by

$$POW_1 = 0.0042 W_T \eta_{HPA} (H_{HP} - H_{CR}) \quad (3.23)$$

where

POW_1 = power produced by the high pressure turbine (MW).

3.4 REHEATER MODELLING

The following assumptions are made:

1. The average values of the parameters like enthalpy, temperature and density are assumed to be the exit values.
2. The steam leaving the Triflex reheater enters the Exit reheater and has the instantaneous properties

of the steam leaving the Triflex reheater.

3. Steam is heated mainly by convection.
4. Reheater tubes are replaced by equivalent control volume across which mass balance energy balance and momentum balance are considered.
5. Heat transfer rate from the flue gases to the tubes is considered constant. This is actually not so, however if the boiler dynamics is also included then this will be determined by that dynamics.

3.4.1 Triflex Reheater

The following equations are used.

Mass Balance

Mass balance across the Triflex reheater is given by the following equation [9]

$$W_{CR} - W_{RO1} = \frac{d\,(\rho_{R1}\, V_{R1})}{dt} \qquad (3.24)$$

where

W_{RO1} = Triflex reheater exit steam flow rate (Kg/Sec.)

ρ_{R1} = density of the steam at the Triflex reheater exit (Kg/m^3),

V_{R1} = steam volume of the Triflex reheater (m^3).

Momentum Balance

The momentum equation describing the steam pressure drop is

$$P_{CR} - P_{RO1} = F_{R1} \left(\frac{W_{CR}^2}{\rho_{R1}} + \frac{L_1}{A_1 g} \right) \frac{d(W_{CR})}{dt} \qquad (3.25)$$

where

F_{R1} = friction factor for the Triflex reheater,

L_1 = effective length of the pipe (m),

A_1 = area of the pipe (m^2).

Substituting the differential term in equation 3.25 from equation 3.17 we get

$$P_{CR} - P_{RO1} = F_{R1} \left(\frac{W_{CR}^2}{\rho_{R1}} + \frac{L_1}{A_1 g} \right) \frac{(1 - C_O) W_T - W_{CR}}{T_O} \qquad (3.26)$$

Energy Balance (Gas Side)

The energy storage in the metal tube walls is given by the following equation [1].

$$Q_{RG1} - Q_{RS1} = C_{TM1} M_1 \frac{d(T_{RM1})}{dt} \qquad (3.27)$$

where

Q_{RG1} = heat flux on the tube walls in Triflex reheater (Kcal/Sec.),

Q_{RS1} = heat added to the steam in the Triflex reheater (Kcal/Sec.),

C_{TM1} = specific heat of the Triflex reheater tube metal (Kcal/Kg ^{o}C),

M_1 = metal mass of the Triflex reheater (Kg),

T_{RM1} = tube metal temperature in the Triflex reheater (^{o}C).

Energy Balance (Steam Side)

The energy balance for steam in the Triflex reheater is given by the following equation

$$\frac{1}{\gamma} \frac{d\,(M_{R1}\, H_{RO1})}{dt} = Q_{RS1} - H_{RO1}\, W_{RO1} + H_{CR}\, W_{CR} \qquad (3.28)$$

where

M_{R1} = effective steam mass in the Triflex reheater (Kg),

γ = ratio of specific heats (C_P/C_V for steam).

Following state relation is determined in terms of Triflex reheater exit pressure P_{RO1} and enthalpy H_{RO1} using empirical fits from the steam tables [16].

$$T_{RS1} = 0.785\,(P_{RO1} - 24.47) + 1.81\,(H_{RO1} - 772.0) + 397 \qquad (3.29)$$

where

T_{RS1} = temperature of steam in the Triflex reheater (^{o}C

The heat added to the steam from the metal walls is given by the following equation [1]

$$Q_{RS1} = C_{RMS1}\,(W_{RO1})^{0.8}\,(T_{RM1} - T_{RS1}) \qquad (3.30)$$

where

C_{RMS1} = a constant to be determined at the initialisation time.

Because of the large volume involved in the reheater there is a storage effect in it. As a result we can consider it as a tank across which changes in flow are approximated by a first order transfer function. The following equation is therefore used

$$\frac{d}{dt}(W_{RI2}) = \frac{W_{CR} - W_{RI2}}{T_7} \qquad (3.31)$$

where

T_7 = time constant associated with the exit reheater (Sec.).

3.4.2 Exit Reheater

The assumptions and arguments made in the case of Triflex reheater, Art. 3.4.1, are valid in this case also and hence will not be restated.

Mass Balance

Mass balance across the exit reheater is given by

$$W_{RI2} - W_{RO2} = \frac{d}{dt}(\rho_{R2} V_{R2}) \qquad (3.32)$$

where

W_{RI2} = steam flow entering the Exit reheater (Kg/Sec.),

W_{RO2} = steam flow at the exit of Exit reheater (Kg/Sec.),

ρ_{R2} = density of steam at Exit reheater exit (Kg/m^3),

V_{R2} = steam volume in the Exit reheater (m^3).

Momentum Balance

Momentum balance describing the steam pressure drop in the Exit reheater is given by the following equation

$$P_{RI2} - P_{RO2} = F_{R2} \frac{W_{RI2}}{\rho_R^2} + \frac{L_2}{A_2 g} \frac{d}{dt} (W_{RI2}) \quad (3.32)$$

where

P_{RI2} = pressure of inlet steam to the Exit reheater (Kg/cm^2),

P_{RO2} = pressure of steam at the exit of Exit reheater (Kg/cm^2),

F_{R2} = friction factor for the Exit reheater,

W_{RI2} = inlet flow rate of steam to the Exit reheater (Kg/sec.),

L_2 = effective length of pipe (m),

A_2 = area of the pipe (m^2).

Energy Balance (Gas Side)

The energy storage in the metal tube walls is given by the following equation

$$Q_{RG2} - Q_{RS2} = C_{TM2} M_2 \frac{d}{dt} (T_{RM2}) \quad (3.34)$$

where

Q_{RG2} = heat flux on the tube walls in Exit reheater (Kcal/sec.),

Q_{RS2} = heat added to the steam in the Exit reheater (Kcal/sec.),

C_{TM2} = specific heat of the Exit reheater tube metal (Kcal/Kg ^{o}C),

M_2 = metal mass of the Exit reheater (Kg),

T_{RM2} = tube metal temperature in the Exit reheater (^{o}C).

Energy Balance (Steam Side)

Energy balance for steam is given by the following equation

$$\frac{1}{\gamma} \frac{d}{dt} (M_{R2} H_{RO2}) = Q_{RS2} + H_{RI2} W_{RI2} - H_{RO2} W_{RO2} \qquad (3.35)$$

where

M_{R2} = effective steam mass in the Exit reheater (Kg),

H_{RI2} = enthalpy of steam entering the Exit reheater (Kcal/Kg),

H_{RO2} = enthalpy of steam coming out of the Exit reheater (Kcal/Kg).

Following state relation is used in determining Exit reheater temperature T_{RS2} by using empirical fits from steam tables [16].

$$T_{RS2} = 0.96 (P_{RO2} - 23.12) + 2.05 (H_{RO2} - 845.0) + 535.0 \qquad (3.35A)$$

The heat added to steam in the Exit reheater is given by the following expression [1]

$$Q_{RS2} = C_{RMS2} (W_{RO2})^{0.8} (T_{RM2} - T_{RS2}) \qquad (3.37)$$

where

C_{RMS2} = a constant to be determined at the time of initialization.

Because of the big reheater volume there is storage effect in the reheater. So we can consider the reheater as a tank across which changes in flow are approximated by a first order transfer function. The following equation is therefore used

$$\frac{d}{dt} (W_{RO2}) = \frac{W_{RI2} - W_{RO2}}{T_8} \qquad (3.38)$$

where

T_8 = time constant associated with the Exit reheater (Sec.).

3.5 MEDIUM PRESSURE TURBINE MODELLING

The medium pressure turbine is considered to consist of four smaller turbines to account for the reduction in flow rate to the succeeding impulse stages on account of extractions at the end of these stages. Extractions are now assumed to take place at the end of each turbine. In addition, inlet flow to the M.P. turbine

is supplemented by attemperation flow to control the temperature. The condition of steam to the MP turbine is therefore modified by the attemperation flow. This is taken care of in the model by using mass balance and energy balance to the attemperator to give the flow conditions at MP turbine inlet.

Inlet flow to the Medium Pressure (M.P.) turbine is given by the following equation:

$$W_{MPI} = W_{RO2} + W_{ATMP} \qquad (3.39)$$

where

W_{MPI} = inlet flow to the M.P. turbine (Kg/sec.),

W_{ATMP} = attemperation flow required to bring the steam to a specified temperature (Kg/sec).

Energy balance for attemperator is given by the expression

$$W_{RO2}\, H_{RO2} = H_{MPI}\, W_{MPI} + W_{ATMP}\, H_{ATMP} \qquad (3.40)$$

where

H_{MPI} = enthalpy of steam entering the M.P. turbine (Kcal/Kg),

H_{ATMP} = enthalpy of the attemperation water (Kcal/Kg).

Once the flow rate to the M.P. turbine is known the down stream conditions can be determined using the same equations as were used in H.P. turbine (Art. 3.3),

thus the flow through each turbine is related to their respective inlet and outlet pressures by following equations [9].

$$W^2_{MPI} = K_2 \rho_{R2} (P_{MPI} - P_{MP1}) \qquad (3.41)$$

where

K_2 = a constant to be determined at the time of initialisation,

P_{MPI} = pressure of steam at the inlet of first M.P. turbine (Kg/cm^2),

P_{MP1} = pressure of steam at the exit of first M.P. turbine (Kg/cm^2).

$$W^2_{MP1} = K_3 \rho_{MP1} (P_{MP1} - P_{MP2}) \qquad (3.42)$$

where

K_3 = a constant to be determined at the time of initialisation,

W_{MP1} = stean flow rate entering the second M.P. turbine (Kg/sec.),

P_{MP2} = pressure of steam at the exit of second M.P. turbine (Kg/cm^2.),

ρ_{MP1} = density of steam at the exit of first M.P. turbine (Kg/m^3).

$$W_{MP2}^2 = K_4 \rho_{MP2} (P_{MP2} - P_{MP3}) \qquad (3.43)$$

where

K_4 = a constant to be determined at the time of initialisation,

W_{MP2} = steam flow rate entering the third M.P. turbine (Kg/sec.),

P_{MP3} = pressure of steam at the exit of third M.P. turbine (Kg/cm^2),

ρ_{MP2} = density of steam at the exit of second M.P. turbine (Kg/m^3).

$$W_{MP3}^2 = K_5 \rho_{MP3} (P_{MP3} - P_{MPO}) \qquad (3.44)$$

where

K_5 = a constant to be determined at the time of initialisation,

W_{MP3} = steam flow rate entering the fourth MP turbine (Kg/sec.),

P_{MPO} = pressure of steam at the exit of fourth M.P. turbine (Kg/cm^2),

ρ_{MP3} = density of steam at the exit of third M.P. turbine (Kg/m^3).

The change in the exit flows as a first order approximation of a change in each turbine inlet flow is described by the following equations:

$$\frac{d}{dt}(W_{MP1}) = \frac{(1 - C_4) W_{MPI} - W_{MP1}}{T_2} \qquad (3.45)$$

where

C_4 = a constant for determining extraction flow,

T_2 = time constant of the first M.P. turbine (sec.),

$$\frac{d}{dt}(W_{MP2}) = \frac{(1 - C_5) W_{MP1} - W_{MP2}}{T_3} \qquad (3.46)$$

where

C_5 = a constant for determining extraction flow,

T_3 = time constant of the second M.P. turbine (sec.).

$$\frac{d}{dt}(W_{MP3}) = \frac{(1 - C_6) W_{MP2} - W_{MP3}}{T_4} \qquad (3.47)$$

where

C_6 = a constant for determining extraction flow,

T_4 = time constant of the third M.P. turbine (Sec.).

$$\frac{d}{dt}(W_{MPO}) = \frac{(1 - C_7) W_{MP3} - W_{MPO}}{T_5} \qquad (3.48)$$

where

C_7 = a constant for determining extraction flow,

T_5 = time constant of the fourth M.P. turbine (sec.).

Expansion of steam in the four turbines is assumed to be isentropic and the following equations are used to determine the isentropic temperatures.

$$T_{MP1} = T_{MPI} \left(\frac{P_{MP1}}{P_{MPI}} \right)^{\frac{n-1}{n}} \qquad (3.49)$$

where

T_{MPI} = temperature of inlet steam to first M.P. turbine (^{o}K),

T_{MP1} = temperature of steam at the exit of first M.P. turbine (^{o}K).

$$T_{MP2} = T_{MP1} \left(\frac{P_{MP2}}{P_{MP1}} \right)^{\frac{n-1}{n}} \qquad (3.50)$$

where

T_{MP2} = temperature of steam at the exit of second M.P. turbine (^{o}K).

$$T_{MP3} = T_{MP2} \left(\frac{P_{MP3}}{P_{MP2}} \right)^{\frac{n-1}{n}} \qquad (3.51)$$

where

T_{MP3} = temperature of steam at the exit of third M.P. turbine (^{o}K).

$$T_{MPO} = T_{MP3} \left(\frac{P_{MPO}}{P_{MP3}} \right)^{\frac{n-1}{n}} \qquad (3.52)$$

where

T_{MPO} = temperature of steam at the exit of fourth M.P. turbine (^{o}K).

The following empirical fits are used to get the enthalpy of steam at the exit of each M.P. turbine.

$$H_{MP1} = -0.35\ P_{MP1} + 0.52\ T_{MP1} + 571.8 \qquad (3.53)$$

where

H_{MP1} = enthalpy of steam at the exit of first M.P. turbine (Kcal/Kg).

$$H_{MP2} = -0.5\ P_{MP2} + 0.51\ T_{MP2} + 580.4 \qquad (3.54)$$

where

H_{MP2} = enthalpy of steam at the exit of second M.P. turbine (Kcal/Kg).

$$H_{MP3} = -0.636\ P_{MP3} + 0.5\ T_{MP3} + 584.5 \qquad (3.55)$$

where

H_{MP3} = enthalpy of steam at the exit of third M.P. turbine (Kcal/Kg).

$$H_{MP0} = -1.36\ P_{MP0} + 0.48\ T_{MP0} + 592.18 \qquad (3.56)$$

where

H_{MP0} = enthalpy of steam at the exit of fourth M.P. turbine (Kcal/Kg).

Efficiency correction factors for the four turbines are determined as follows:

$$\eta_{F1} = \frac{(\frac{W_{MP1}}{W_R}) - W_L}{(\frac{W_{MP1}}{W_R})(1 - W_L)} \qquad (3.57)$$

where

η_{F1} = efficiency correction factor for first M.P. turbine,

$$\eta_{F2} = \frac{(\frac{W_{MP2}}{W_R}) - W_L}{(\frac{W_{MP2}}{W_R})(1 - W_L)} \tag{3.58}$$

where

η_{F2} = efficiency correction factor for second M.P. turbine.

$$\eta_{F3} = \frac{(\frac{W_{MP3}}{W_R}) - W_L}{(\frac{W_{MP3}}{W_R})(1 - W_L)} \tag{3.59}$$

where

η_{F3} = efficiency correction factor for third M.P. turbine.

$$\eta_{F4} = \frac{(\frac{W_{MPO}}{W_R}) - W_L}{(\frac{W_{MPO}}{W_R})(1 - W_L)} \tag{3.60}$$

where

η_{F4} = efficiency correction factor for fourth M.P. turbine.

The actual efficiencies are determined by the following expressions

$$\eta_{MP1} = \eta_{MP}\ \eta_{F1} \tag{3.61}$$

where

η_{MP1} = actual efficiency of the first M.P. turbine,

η_{MP} = thermodynamic efficiency of each M.P. turbine.

$$\eta_{MP2} = \eta_{MP} \ \eta_{F2} \tag{3.62}$$

where

η_{MP2} = actual efficiency of the second MP turbine,

$$\eta_{MP3} = \eta_{MP} \ \eta_{F3} \tag{3.63}$$

where

η_{MP3} = actual efficiency of the third M.P. turbine.

$$\eta_{MP4} = \eta_{MP} \ \eta_{F4} \tag{3.64}$$

where

η_{MP0} = actual efficiency of the fourth M.P. turbine.

Actual enthalpy of steam is determined using the following equations.

$$H_{MP1A} = H_{MPI} - \eta_{MP1} (H_{MPI} - H_{MP1}) \tag{3.65}$$

where

H_{MP1A} = actual enthalpy of steam at the first M.P. turbine exit (Kcal/Kg).

$$H_{MP2A} = H_{MP1A} - \eta_{MP2} (H_{MP1A} - H_{MP2}) \tag{3.66}$$

where

H_{MP2A} = actual enthalpy of steam at the exit of second M.P. turbine (Kcal/Kg).

$$H_{MP3A} = H_{MP2A} - \eta_{MP3} (H_{MP2A} - H_{MP3}) \tag{3.67}$$

where

H_{MP3A} = actual enthalpy of steam at the exit of third M.P. turbine (Kcal/Kg).

$$H_{MPOA} = H_{MP3A} - \eta_{MPO} (H_{MP3A} - H_{MPO}) \quad (3.68)$$

where

H_{MPOA} = actual enthalpy of steam at the exit of fourth M.P. turbine (Kcal/Kg).

Power generated by each turbine is given by the following expressions:

$$POW_2 = 0.0042 W_{MPI} \eta_{MP1} (H_{MPI} - H_{MP1}) \quad (3.69)$$

where

POW_2 = power produced by the first M.P. turbine (MW),

$$POW_3 = 0.0042 W_{MP1} \eta_{MP2} (H_{MP1A} - H_{MP2}) \quad (3.70)$$

where

POW_3 = power produced by the second M.P. turbine (MW),

$$POW_4 = 0.0042 W_{MP2} \eta_{MP3} (H_{MP2A} - H_{MP3}) \quad (3.71)$$

where

POW_4 = power produced by the third M.P. turbine (MW),

$$POW_5 = 0.0042 W_{MP3} \eta_{MP4} (H_{MP3A} - H_{MPO}) \quad (3.72)$$

where

POW_5 = power produced by the fourth M.P. turbine (MW).

3.6 LOW PRESSURE TURBINE MODELLING

Exit steam from this turbine goes to the condenser. Extractions are lumped into one extraction and this extraction is assumed to take place at the end of this turbine. Further condenser pressure is assumed to be constant.

The change in the Low Pressure (L.P.) turbine exit flow is assumed as a first order approximation of the inlet flow and is given by the following equation

$$\frac{d}{dt}(W_{LPO}) = \frac{(1 - C_8)\, W_{MPO} - W_{LPO}}{T_6} \tag{3.73}$$

where

W_{LPO} = outlet flow from the L.P. turbine (Kg/sec.),

T_6 = time constant of the L.P. turbine (sec.).

In addition efficiency correction factor, enthalpy of steam at the exit of L.P. turbine and power produced by the L.P. turbine are given by the following expressions.

$$\eta_{F5} = \frac{(\frac{W_{LPO}}{W_R}) - W_L}{(\frac{W_{LPO}}{W_R})\,(1 - W_L)} \tag{3.74}$$

where

η_{F5} = efficiency correction factor for the L.P. turbine.

$$\eta_{LPA} = \eta_{LP}\ \eta_{F5} \tag{3.75}$$

where

η_{LPA} = actual efficiency of the L.P. turbine,

η_{LP} = thermodynamic efficiency of the L.P. turbine.

$$H_{LPOA} = H_{MPOA} - \eta_{LPA}\,(H_{MPOA} - H_{LPO}) \tag{3.76}$$

where

H_{LPOA} = actual enthalpy of steam at the exit of L.P. turbine (Kcal/Kg),

H_{LPO} = ideal enthalpy of steam at the exit of L.P. turbine (Kcal/Kg).

Power produced is given by the following expression,

$$POW_6 = 0.0042\, W_{MPO}\, \eta_{LPA}\, (H_{MPOA} - H_{LPO}) \quad (3.77)$$

where

POW_6 = power produced by the L.P. turbine (MW).

3.7 CONDENSER MODELLING

It is assumed that condenser pressure remains constant. Heat rejected by the condensing steam is therefore determined by the quantity of condensing steam.

Heat flow rate from metal to cooling water is given by the following expression [1].

$$Q_{MW} = C_{CMW}\, (W_{CW})^{0.6}\, (T_{CM} - T_{CW}) \quad (3.78)$$

where

Q_{MW} = heat flow rate from metal to cooling water in condenser (Kcal/sec.),

C_{CMW} = a constant determined at initialisation time,

W_{CW} = quantity of cooling water (Kg/sec.),

T_{CM} = temperature of condenser metal (^{o}C),

T_{CW} = temperature of the cooling water (^{o}C).

Enthalpy at the condenser exit is determined by an energy balance equation and is given by the following expression

$$H_{CO} = H_{LPO} - Q_{SM} / W_{LPO} \qquad (3.79)$$

where

H_{CO} = enthalpy of water at the condenser exit (Kcal/kg),

Q_{SM} = heat rejected by steam to the cooling water.

Energy storage in the metal walls is given by the following equation

$$Q_{SM} - Q_{MW} = C_{CM} M_3 \frac{d}{dt} (T_{CM}) \qquad (3.80)$$

where

C_{CM} = specific heat of the condensor metal (Kcal/Kg ^{o}C)

M_3 = condenser metal mass (Kg).

3.8 LOW PRESSURE (L.P.) AND HIGH PRESSURE (H.P.) HEATER MODELLING

The feed water heaters are considered seperately to take into account the fact that extraction rates are different and they have different heat contents. For each feed water heater, energy storage in the metal tube walls, heat transfer rate from metal tube to feed water are considered and thus the enthalpy of feed water coming out of the heater is determined.

3.8.1 Low Pressure Feed Water Heater No. 1

Energy storage in the metal walls of the feed water heater No. 1 is given by the following equation

$$Q_{LH1SM} - Q_{LH1MW} = C_{HM1} M_4 \frac{d}{dt} (T_{HM1}) \qquad (3.81)$$

where

Q_{LH1SM} = heat transfer rate from the steam to metal in the first L.P. feed water heater (Kcal/sec.),

Q_{LH1MW} = heat transfer rate from metal to feed water in the first L.P. feed water heater (Kcal/sec.),

C_{HM1} = specific heat of the tube metal in the first L.P. feed water heater (Kcal/Kg ^{o}C),

M_4 = first L.P. feed water heater metal mass (Kg),

T_{HM1} = first L.P. feed water heater metal temperature (^{o}C).

Metal to feed water heat transfer rate in the heater is given by the following equation [1].

$$Q_{LH1MW} = C_{HMW1} (W_{LH1})^{0.6} (T_{HM1} - T_{HW1}) \qquad (3.82)$$

where

C_{HMW1} = a constant to be determined at initialisation time,

W_{LH1} = feed water flow rate through the first L.P. feed water heater (Kg/sec.),

T_{HW1} = feed water temperature in the first L.P. feed water heater (^{o}C)

Enthalpy of feed water coming out of the first feed water heater is determined by

$$H_{LH10} = H_{CO} + Q_{LH1MW} / W_{LH1} \qquad (3.83)$$

where

H_{LH10} = enthalpy of feed water coming out of the first feed water heater (Kcal/Kg).

3.8.2 Low Pressure Feed Water Heater No. 2 Modelling

Energy storage in the tube metal walls is given by following equation

$$Q_{LH2SM} - Q_{LH2MW} = C_{HM2} \cdot M_5 \cdot \frac{d}{dt} (T_{HM2}) \qquad (3.84)$$

where

Q_{LH2SM} = heat transfer rate from steam to metal in second L.P. feed water heater (Kcal/Sec.),

Q_{LH2MW} = heat transfer rate from metal to water in the second L.P. feed water heater (Kcal/Sec.)

C_{HM2} = specific heat of the tube metal in second L.P. feed water heater (Kcal/Kg ^{o}C),

M_5 = second L.P. feed water heater metal mass (Kg.)

T_{HM2} = second L.P. feed water heater metal temperature (^{o}C).

Metal to feed water heat transfer rate in the heater is given by following expression. [1]

$$Q_{LH2MW} = C_{HMW2} \cdot (W_{LH2})^{0.6} \cdot (T_{HM2} - T_{HW2}) \qquad (3.85)$$

where

C_{HMW2} = a constant to be determined at initialisation time,

W_{LH2} = feed water flow rate through the second L.P. feed water heater (Kg/Sec.)

T_{HW2} = feed water temperature in the second L.P. feed water heater (^{o}C)

Enthalpy of feed water coming out of the second feed water heater is determined by

$$H_{LH20} = H_{LH10} + Q_{LH2MW} / W_{LH2} \qquad (3.86)$$

where

H_{LH20} = enthalpy of feed water coming out of the second feed water heater (Kcal/Kg)

3.8.3 Low Pressure Feed Water Heater No. 3 Modelling

Energy storage in the tube metal walls is given by following expression

$$Q_{LH3SM} - Q_{LH3MW} = C_{HM3} \cdot M_6 \cdot \frac{d}{dt} (T_{HM3}) \qquad (3.87)$$

where

Q_{LH3SM} = heat transfer rate from steam to metal in the third L.P. feed water heater (Kcal/Sec.),

Q_{LH3MW} = heat transfer rate from metal to water in the third L.P. feed water heater (Kcal/Sec.),

C_{HM3} = specific heat of the tube metal in the third L.P. feed water heater (Kcal/Kg ^{o}C)

M_6 = third L.P. feed water heater metal mass (Kg.)

T_{HM3} = metal temperature in the third L.P. feed water heater (^{o}C)

Metal to feed water heat transfer rate in the third heater is given by following expression [11]

$$Q_{LH3MW} = C_{HMW3} \cdot (W_{LH3})^{0.6} \cdot (T_{HM3} - T_{HW3}) \qquad (3.88)$$

where

C_{HMW3} = a constant to be determined at initialisation time,

W_{LH3} = feed water flow rate through the third L.P. feed water heater (Kg/Sec.)

T_{HW3} = feed water temperature in the third L.P. feed water heater (^{o}C)

Enthalpy of feed water coming out of third feed water heater is determined by the following expression

$$H_{LH30} = H_{LH20} + Q_{LH3MW} / W_{LH3} \qquad (3.89)$$

where

H_{LH30} = enthalpy of feed water coming out of the third L.P. feed water heater (Kcal/Kg).

3.8.4 Low Pressure Feed Water Heater No. 4 Modelling

Energy storage in the tube metal walls is given by the following expression

$$Q_{LH4SM} - Q_{LH4MW} = C_{HM4} \cdot M_7 \cdot \frac{d}{dt}(T_{HM4}) \qquad (3.90)$$

where

Q_{LH4SM} = heat transfer rate from steam to metal in the fourth L.P. feed water heater (Kcal/Sec.),

Q_{LH4MW} = heat transfer rate from metal to water in the fourth L.P. feed water heater (Kcal/Sec.),

C_{HM4} = specific heat of the tube metal in the fourth L.P. feed water heater (Kcal/Kg ^{o}C),

M_7 = fourth L.P. feed water heater metal mass (Kg),

T_{HM4} = metal temperature in the fourth L.P. feed water heater (^{o}C)

Metal to feed water, heat transfer rate in the fourth heater is given by the following expression [1]

$$Q_{LH4MW} = C_{HMW4} \cdot (W_{LH4})^{0.6} \cdot (T_{HM4} - T_{HW4}) \qquad (3.91)$$

where

C_{HMW4} = a constant to be determined at initialisation time,

W_{LH4} = feed water flow rate through the fourth L.P. feed water heater (Kg/Sec.),

T_{HW4} = feed water temperature in the fourth L.P. feed water heater (^{o}C).

Enthalpy of feed water coming out of the fourth heater is determined by the following expression

$$H_{LH40} = H_{LH30} + Q_{LH4MW} / W_{LH4} \qquad (3.92)$$

where

H_{LH40} = enthalpy of feed water coming out of the fourth L.P. feed water heater (Kcal/Kg).

3.8.5 High Pressure Feed Water Heater No. 1 Modelling

Heat energy storage in the metal tube wall is given by the following expression

$$Q_{HH1SM} - Q_{HH1MW} = C_{HM5} \cdot M_8 \cdot \frac{d}{dt} (T_{HM5}) \qquad (3.93)$$

where

Q_{HH1SM} = heat transfer rate from steam to metal in the first H.P. feed water heater (Kcal/Sec.),

Q_{HH2MW} = heat transfer rate from metal to water in the first H.P. feed water heater (Kcal/Sec.),

C_{HM5} = specific heat of the tube metal in the first H.P. feed water heater (Kcal/Kg ^{o}C),

M_8 = first H.P. feed water heater metal mass (Kg.),

T_{HM5} = first H.P. feed water heater metal temperature (^{o}C).

Metal to feed water, heat transfer rate in the first H.P. heater is given by the following equation [1].

$$Q_{HH1MW} = C_{HMW5} \cdot (W_{HH1})^{0.6} \cdot (T_{HM5} - T_{HW5})$$

where

C_{HMW5} = a constant to be determined at initialisation time,

W_{HH1} = feed water flow rate through the first H.P. feed water heater (Kg/Sec.),

T_{HW5} = feed water temperature in the first H.P. feed water heater (^{o}C).

Enthalpy of feed water coming out of the first H.P. heater is determined by the following expression

$$H_{HH10} = H_{LH40} + Q_{HH1MW} / W_{HH1} \qquad (3.95)$$

where

H_{HH10} = enthalpy of feed water coming out of the first H.P. feed water heater (Kcal/Kg).

3.8.6 High Pressure Feed Water Heater No. 2 Modelling

Heat energy storage in the metal walls is given by the following expression

$$Q_{HH2SM} - Q_{HH2MW} = C_{HM6} \cdot M_9 \cdot \frac{d}{dt}(T_{HM6}) \qquad (3.96)$$

where

Q_{HH2SM} = heat transfer rate from steam to metal in the second H.P. feed water heater (Kcal/Sec.),

I.I.T. KANPUR
CENTRAL LIBRARY
Acc. No. 55421

Q_{HH2MW} = heat transfer rate from metal to water in the second H.P. feed water heater (Kcal/Sec.),

C_{HM6} = specific heat of the tube metal in the second H.P. feed water heater (Kcal/Kg ^{o}C),

M_g = second H.P. feed water heater metal mass (Kg),

T_{HM6} = second H.P. feed water heater metal temperature (^{o}C).

Metal to feed water heat transfer rate in the second H.P. heater is given by the following equation [11].

$$Q_{HH2MW} = C_{HMW6} \cdot (W_{HH2})^{0.6} \cdot (T_{HM6} - T_{HW6}) \qquad (3.97)$$

where

C_{HMW6} = a constant to be determined at initialisation time,

W_{HH2} = feed water flow rate through the second H.P. feed water heater,

T_{HW6} = feed water temperature in the second H.P. feed water heater (^{o}C).

Enthalpy of feed water coming out of the second H.P feed water heater is given by the following equation

$$H_{HH20} = H_{HH10} + Q_{HH2MW} / W_{HH2} \qquad (3.98)$$

where

H_{HH20} = enthalpy of feed water coming out of the second feed water heater (Kcal/Kg).

3.8.7 Model Structure

The structure of non-linear ordinary differential equations is of the type

$$\dot{\bar{X}} = f (\bar{X}, \bar{Y}, \bar{U}) \qquad (3.99)$$

where $\bar{x}$ is the state vector given by

$$\bar{X}^T = (W_{CR}, \ ^{\epsilon}_{R1}, H_{RO1}, T_{RM1}, W_{RI2}, \ ^{\epsilon}_{R2}, H_{RO2}, W_{RO2}, T_{RM2}, W_{MP1}, W_{MP2}, W_{MP3}, W_{MPO}, T_{CM}, T_{HM1}, T_{HM2}, T_{HM3}, T_{HM4}, T_{HM5}, T_{HM6})$$

$\bar{Y}$ the auxilliary variables are given by

$$\bar{Y} = \underline{G} (\bar{X}, \bar{U}) \qquad (3.100)$$

$\bar{U}$ is the control vector defined by

$$\bar{U}^T = (W_T, Q_{RG1}, Q_{RG2})$$

Substituting for $\bar{Y}$ from equation (3.100) in equation (3.99) we get the equation (3.99) as

$$\dot{\bar{X}} = F (\bar{X}, \bar{U}) \qquad (3.101)$$

where F denotes the new functional dependence.

For the above set of equations a computer program was developed and these equations were solved on a digital computer (IBM 7044) using the Runga-Kutta integration technique. The transient responses of the turbine system for step changes in few control parameter were obtained and have been discussed in the next chapter.

CONCLUSIONS

In this chapter the dynamic model of the turbine unit using physical laws and empirical relations was developed. It yielded 22 first order differential equations alongwith 77 algebraic equations to represent the turbine unit. The above system of equations was solved in a digital computer and responses obtained will be presented in Chapter 4.

CHAPTER 4

RESULTS

4.1 INITIALISATION

Mathematical model for the Panki turbine was presented in Chapter 3. Before any transient study is conducted on the model the steady state of the model has to be obtained for given input conditions. This is called as initialisation.

The constants used in the equations are determined using the steady state values of parameters at 90 MW and are given in Appendix 1. For any given input condition there are two methods for determining the steady state of the model. In the first method the $\dot{X}$ term of equation 3.99 is equated to zero and the resulting nonlinear algebraic equations are solved by any suitable numerical elimination technique. In the second method, the steady state data obtained from the plant is used as a starting point in the integration scheme. The second method is used in the present study. As mentioned earlier, steady state data at 90 MW was available from the plant and this was used to determine the model constants. It can be pointed out here that generally the actual steady state data obtained from the plant may not be the same as that given by the model. However, in the present case, as

the steady state constants of the model were determined from the plant data, the model steady state is same as the plant steady state. Fourth order Runga-Kutta method is used for the integration and the integration scheme is terminated when the difference in the successive values of the state variables is reduced to less than 1% of the previous values. Steady state operating values of the model are determined for many loads and are presented for the case of the governing stage. In one case, for which the plant data was available, comparison has been made with the plant data. Transient tests are carried out for two cases. First, for the 10 MW load drop from 90 MW level and second for a step change in gas to metal heat transfer rates in the Triflex and Exit reheater.

4.2 STEADY STATE RESULTS

Table 4.1 shows the model steady state values obtained for 70, 80, 90, 100 and 110 MW loads. The parameters shown are pressures and temperatures after the three throttle valves (P_{TH1}, P_{TH2}, P_{TH3}, T_{TH1}, T_{TH2}, T_{TH3}) obtained for the governing stage after implementing the flow chart shown in Figure 4. As the load increases the pressure after the three throttle valvesalso increases. This is explained by the fact that with an increase in load the throttle valve opening also starts becoming

larger and larger and as a result the pressure drop. across the throttle valve decreases. This has been shown in Table 4.2. Further, for any one particular load, the pressure after the first throttle valve will have a higher value than the second and the second will have a higher value than for the third. This is so because the first valve starts opening the earliest and as such at any particular load it will have a larger opening than the second and similarly the second valve will have a larger opening than the third. The temperatures after the throttle valves also show the same trend and are presented in Table 4.1.

TABLE 4.1

PRESSURES AND TEMPERATURES AFTER THROTTLE VALVE FOR DIFFERENT LOADS

PARAMETER / LOAD	70	80	90	100	110
P_{TH1}	78.27	92.66	102.05	118.79	130.0
P_{TH2}	68.78	81.40	88.55	109.99	118.66
P_{TH3}	NOT OPEN	NOT OPEN	NOT OPEN	107.19	115.49
T_{TH1}	515.00	520.70	524.50	531.20	535.00
T_{TH2}	511.20	516.10	519.10	527.60	531.00
T_{TH3}	NOT OPEN	NOT OPEN	NOT OPEN	526.50	529.80

TABLE 4.2

DROP ACROSS THE VALVES FROM CONSTANT INLET PRESSURE OF 130 KG/CM^2

PARAMETER / LOAD (MW)	70	80	90	100	110
P_{TH1}	51.73	37.34	22.0	11.21	0
P_{TH2}	61.20	49.00	41.5	20.00	11.4
P_{TH3}	NOT OPEN	NOT OPEN	NOT OPEN	23.00	15.0

The governing stage pressure P_{HP} and temperature T_{HP} have been determined for different loads and are presented in Table 4.3. The steady state value of P_{HP} at various loads has been compared with plant steady state value at these loads in the same table.

TABLE 4.3

GOVERNING STAGE PRESSURE AT VARIOUS LOADS

PARAMETER	LOAD (MW)	70	80	90	100	110
P_{HP}	MODEL	68.04	80.10	86.97	107.13	115.14
	PLANT	72.00	82.00	86.07	104.00	114.00
T_{HP}	MODEL	499.60	504.20	505.75	518.70	521.50

The steady state values of the state variables obtained from the model at 90 MW are listed below in Table 4.4.

TABLE 4.4

STEADY STATE VALUES OF STATE VARIABLES FOR 90 MW

S.No.	STATE VARIABLE		STEADY STATE VALUE
1	W_{CR}	Kg/Sec.	74.00
2	ρ_{R1}	Kg/m^3	7.88
3	H_{RO1}	Kcal/Kg	771.00
4	T_{RM1}	^oC	460.00
5	W_{RI2}	Kg/Sec.	74.00
6	ρ_{R2}	Kg/m^3	6.20
7	H_{RO2}	Kcal/Kg	844.00
8	W_{RO2}	Kg/Sec.	74.00
9	T_{RM2}	^oC	590.00
10	W_{MP1}	Kg/Sec.	72.50
11	W_{MP2}	Kg/Sec.	70.50
12	W_{MP3}	Kg/Sec.	68.80
13	W_{MPO}	Kg/Sec.	65.60
14	W_{LPO}	Kg/Sec.	61.88
15	T_{CM}	^oC	45.00
16	T_{HM1}	^oC	110.00

Continued

S.No.	STATE VARIABLE		STEADY STATE VALUE
17	T_{HM2}	^{o}C	143.00
18	T_{HM3}	^{o}C	220.00
19	T_{HM4}	^{o}C	315.00
20	T_{HM5}	^{o}C	450.00
21	T_{HM6}	^{o}C	348.00

DISCUSSION

The comparison of governing stage exit pressure determined by model to the plant data is shown in Table 4.3 The difference in the two values is highest at 5.5% for 70 MW load. At 80 MW the difference is 2.4% on the lower side. For 90 MW both model and plant values nearly match. This is due to the fact that the model constants were determined using the steady state values at 90 MW. At 100 MW the difference in model and plant values is at 2.8% on higher side and there is a mismatch of only 0.7% at 110 MW load. The error increases as the load value moves down from the 90 MW level. On the higher side this trend is not reflected. This can be due to various assumptions, simplifications and guesses made wherever the plant physical constants were not available.

4.3 TRANSIENT RESPONSES

4.3.1 Plant Responses For a Load Drop of 10 MW From the Steady State at 90 MW

A plant test was conducted on the second 110 MW unit of the Panki Thermal Power Station, Kanpur. First, when the plant was operating at steady state at 90 MW, various control loops were put on manual i.e. the plant was put on open loop. Then, the load setting was reduced by 10 MW. All the indicators available in the control room were observed by a group of 20 persons with one person taking down the reading for each indicator. The readings were taken manually at a time interval of 2 sec. up to 20 sec. then at a interval of 5 sec. up to 5 minutes. Various recorder charts that were operative in the control room were also obtained. Out of these, few parameters are compared with model tests. It can be pointed out here that very little instrumentation was available on the turbine side. Further, the instrument calibration was not checked before the test and many persons taking down the readings of the indicators were not experienced in this sort of work. Hence the results obtained from plant test can only act as guide line.

4.3.2 Model Response For A Load Drop of 10 MW From Steady State of 90 MW

The model responses for a load drop of 10 MW are discussed in the following articles. For obtaining these,

the total input flow to turbine, W_T was decreased by a step to its new value at 80 MW.

4.3.2.1 High Pressure Turbine

A drop from 90 MW to 80 MW in load results in a step decrease in the input flow to the turbine. The responses obtained for the outlet flow from H.P. turbine are shown in Fig. 10. The outlet flow from the turbine (W_{CR}) takes time (equal to its time constant) for adjusting to the new value of W_T. This has been brought out in Fig. 10a. The turbine outlet pressure undergoes a rapid change in pressure as is evident from equation 3.16. The response obtained for this pressure from the plant tests is compared with the model response in Fig. 10b. As is evident from figure the pressure in the plant stabilises at a higher value than the model. This can be due to some error in instrumentation or in observing the readings of the indicators due to the inexperience of the observer. The temperature of the outlet steam from the H.P. turbine follows the same trend as the pressure (Fig. 10c). This happens because the temperature at outlet of the turbine depends on the inlet pressure and temperature both of which fall down very rapidly with a decrease in load.

4.3.2.2 Triflex and Exit Reheater Responses

The responses obtained for the two reheaters are shown in Figure 11. Figure 11a shows the variation of Triflex reheater outlet flow. The flow, W_{RO1}, starts going down rapidly and by 6 sec. it becomes more or less stable. This is evident from equation 3.31. Because of the large volume involved in a reheater, it behaves like a storage tank. The pressure after the first reheater P_{RO1} also decreases as shown in Figure 11b. This is explained by the following argument. P_{RO1} is dependent on the inlet pressure to the reheater, the flow and the density. The inlet pressure to the reheater goes down fast because of the part played by the H.P. turbine dynamics. Further, because of the drop in flow, W_{RO1}, there is storage effect in the reheater as a result of which the density goes down. Combined effect of these results in a gradual decrease of pressure. Figure 11c shows the response of the heat transfer rate from metal to steam (Q_{RS1}). As the flow passing through the reheater goes down the heat added to the steam from the metal starts going down due to reduction in convective heat transfer as a result of decrease in steam velocity. This gives rise to two effects. First the heat stored in the metal walls goes up which results in an increase in the reheater metal temperature, second because of the less heat being added to the steam now, the temperature of

steam T_{RS1} starts going down. Both these effects tend to increase the heat transfer rate Q_{RS1}. As a result first Q_{RS1} starts going down because of the dominant effect of flow decrease and then this downward trend is slowed down due to the effects that the metal temperature and steam temperature exercise on Q_{RS1}. After the flow has stabilised around 6 seconds, its effect on the Q_{RS1} vanishes and because the metal temperature and steam temperature take little more time to stabilise there is a marginal increase in the heat transfer rate Q_{RS1}. The steam temperature T_{RS1} follows the trend shown by Q_{RS1} (Fig. 11d). The steam density response has been shown in Fig. 11e.

The Exit reheater outlet flow behaves the same way as the Triflex reheater outlet flow. This Exit reheater outlet flow first goes down and then stabilises after 7 secs. This is shown in Fig. 11f. The outlet pressure of the Exit reheater also shows the same response as that of the Triflex reheater. In this case response for comparision to plant test was available and both have been drawn in Fig. 11g. The plant test response shows a slower decrease than the model response up to 1 sec. and then both show a appreciable fall in the rate of decrease. Exact matching was not obtained due to the same reasons as mentioned earlier. The metal to steam heat transfer rate Q_{RS2} responds in a way shown in Fig. 11h. The sharp rate of decrease, unlike

the Triflex reheater case, can be attributed to the fact that tube metal mass in the Exit reheater is larger than the Triflex reheater and the metal temperature increase effect due to heat storage in the metal walls, which tends to increase the heat transfer rate, goes down. As a result there is no restraint on Q_{RS2} initially. But this decrease of Q_{RS2} gives rise to steam temperature decrease which in turn tries to increase the heat transfer rate. The enthalpy at the exit of second reheater follows a very similar trend as shown in Fig. 11i.

4.3.2.3 Medium Pressure Turbine

The responses obtained for the medium pressure turbine are shown in Fig. 12. The flow at the outlet of first M.P. turbine responds in a way shown in Fig. 12a. This flow decreases with the decrease of inlet flow to the turbine. The time constants of the individual M.P. turbine are of the order of 1 sec. which is very small compared to reheater time constant and as a result the flow response W_{MP1} is nearly the same as that of the second reheater. The pressure at the exit of the first M.P. turbine is affected by the inlet pressure to the turbine, the flow passing through it and the density of the steam. The pressure first goes down because of the effect of the decrease in inlet pressure to the medium pressure turbine, but as flow also

goes down and there is only a marginal decrease in the steam density, the pressure goes up as can be seen from equation 3.41. The temperature of steam at the exit of first M.P. turbine follows a similar trend due to its dependence on pressure and also due to the effect of second reheater enthalpy variation (Fig. 12c).

The second M.P. turbine behaves in the same way as the first M.P. turbine. Flow response is shown in Fig. 12d. There is no noticeable difference in the response from the first one, a fact, which is corroborated by the low time constant of the M.P. turbine. The response for pressure is shown in Fig. 12e and the temperature response is shown in Fig. 12f. The trends are similar to the ones obtained for the first M.P. turbine.

The third M.P. turbine also behaves like the first two M.P. turbines and responses are plotted in Fig. 12g, 12h and 12i. Figure 12g shows the outlet flow response. It also shows no noticeable difference in the dynamics because of the low time constant and the large time scale which had to be used for this. Outlet pressure response has been shown in Fig. 12h and the outlet temperature response is shown in Fig. 12i.

The fourth M.P. turbine responds in a similar way as the first three ones and the outlet flow, pressure and temperature responses are given by figures 12j, 12k, and 12l respectively.

4.3.2.4 Condenser and Feedwater Heaters

Figures 13a to 13g show the responses in metal to water heat transfer rates for condenser, low pressure feed water heater No. 1, 2, 3, 4 and the high pressure feed water heater Nos. 1 and 2, respectively. All show a decreasing trend which can be explained by the fact that as the load is decreased the quantity of steam extracted also goes down. As a result less steam condenses on the tubes resulting in lesser heat transfer to the feed water passing through these tubes. The metal temperatures of the tubes in the feed water heaters and condenser do not change much because of the thin tube thickness.

4.3.3 Model Responses For 20 Percent Increase in Heat Transfer Rate In ReheatersFrom Flue Gases

In another transient study conducted, the heat transfer rate to the tube metal walls from the flue gases is increased by 20% step. The responses obtained for this are shown in Fig. 14. Figures 14a, 14b and 14c show the responses of metal to steam heat transfer rate, steam enthalpy and metal temperature for the Triflex reheater. As the heat transfer rate from gas to metal is increased by a step the tube metal temperature also increases slowly due to the large metal mass involved. This increase in metal temperature increases the heat transfer rate to the steam

from the metal Q_{RS1}. This is brought out by the Fig. 14a. The metal temperature variation is shown in Fig. 14c. The increase in heat content of the steam is evident in the response of steam enthalpy (Fig. 14b). Similar responses are obtained for the Exit reheater and are shown in Fig. 14d, 14e and 14f. The Exit reheater metal temperature increases more slowly than the Triflex reheater because the metal mass in the Exit reheater is approximately two and half times that of the Triflex reheater. This trend of slow rise in metal temperature is reflected in the metal to steam heat transfer rate and the steam enthalpy. Other parameters downstream of the reheater do not show substantial variation in their values but a marginal increase in downstream enthalpies and power produced by the turbine is noticed (not shown in figure).

4.3.4 Future Work Suggested

In the present study the model of the turbine for a 110 MW unit is developed. Model for the boiler of the unit was developed earlier [1]. The next obvious step would be to combine these two models and to incorporate various control schemes in the model. Once this is done many meaningful tests can be conducted on the plant and the responses can be compared with the model. Then the model could be used to decide the control strategies and their evaluation. Further, the complete model can be used for designing higher capacity units by scaling it up.

REFERENCES

1. C.N. Srinivasan, M.Tech. Thesis, Department of Mech. Engg., I.I.T. Kanpur (1977).
2. K.L. Chien, E.I. Ergin, C. Ling and A. Lee, "Dynamic Analysis of a Boiler", Trans. ASME, Vol. 80, pp. 1809 - 1819 (1958).
3. J.H. Daniels, M. Enns, R.D. Hottenstine, "Dynamic Representation of a Large Boiler Turbine Unit", ASME Paper No. 61 - SA - 69, ASME Summer Annual Meeting (1961).
4. F.T. Thompson, "A Dynamic Model of a Drum Type Boiler System", IEEE Trans. PAS, Vol. 86, pp. 625 - 635, (1967).
5. H.G. Dallas, D.M. Sauter, "Field Testing For Verification of a Dynamic Model", ASME Paper 61 - SA - 68, ASME Summer Annual Meeting (1961).
6. IBM Interim Report, "Power System Computer Feasibility Study", Vol. II, Research Division, San Jose, California (1968).
7. J.P. McDonald, H.G. Kwatny, J.H. Spare, "Non-Linear Model of a Reheat Boiler-Turbine-Generator System", Philadelphia Electric Co., Research Division Report No. 196 (1970).

8. J.P. McDonald, H.G. Kwatny, J.H. Spare, "A Non-Linear Model For Reheat Boiler-Turbine Generator Systems, Part I - General Description and Evaluation," in Proc. 12th Joint Automatic Control Conf., 1971, pp. 219 - 226.

9. J.P. McDonald, H.G. Kwatny, J.H. Spare, "A Non-Linear Model For Reheat Boiler-Turbine-Generator Systems, Part II - Development," in Proc. 12th Joint Automatic Control Conf, 1971, pp. 227 - 236.

10. W.J. Kearton, "Steam Turbine Theory and Practice," MLBS. Pitman, London (1902).

11. A Ralston and H.S. Wilfe, "Mathematical Methods For Digital Computers," Wiley New York, (1967).

12. BHEL Plant Data Manual for 110 MW Unit, Panki Thermal Power Station, Kanpur.

13. BHEL Maintenance Manual For 110 MW Unit, Panki Thermal Power Station, Kanpur.

14. I.L. Kota Instrumentation Manual, Panki Thermal Power Station, Kanpur.

15. Panki Thermal Power Station Plant Drawings No. 9, 10, 11, Prepared by Development Consultants Pvt. Ltd.

16. ISI Steam Tables, Indian Standard Institution, Edition 1, 1966.

APPENDIX - 1

PLANT DATA

The following data has been taken from the plant manuals.

Steam pressure at the inlet of the throttle valve	= 130 Kg/cm^2
Steam temperature at the inlet of throttle valve	= 535 ^oC
Steam density at the inlet of throttle valve	= 37.8 Kg/m^3
Steam enthalpy at the inlet of throttle valve	= 819.8 Kcal/k
Number of throttle valves	= 4
Number of nozzles in the first nozzle ring	= 8
Number of nozzles in the second nozzle ring	= 8
Number of nozzles in the third nozzle ring	= 7
Number of nozzles in the fourth nozzle ring	= 7
Number of stages in the high pressure turbine	= 8
Number of stages in the medium pressure turbine	= 12
Number of stages in the low pressure turbine	= 4 on each side
Number of low pressure feed water heaters	= 5
Number of high pressure feed water heaters	= 2
Number of tubes in the Triflex reheater	= 160
Number of tubes in the Exit reheater	= 224
Heating surface available for Triflex reheater	= 850 m^2
Heating surface available for Exit reheater	= 1714 m^2
Effective steam volume in the Triflex reheater	= 11.6 m^2

Effective steam volume in the Exit reheater	=	39.1 m^3
Tube metal mass in the Triflex reheater	=	10.33 Tons
Tube metal mass in the Exit reheater	=	30.59 Tons
Maximum design metal temperature of Triflex reheater	=	460 ^oC
Maximum design metal temperature of Exit reheater	=	590 ^oC
Outside diameter of Triflex reheater tubes	=	70 mm
Outside diameter of Exit reheater tubes	=	60.3 mm
Triflex reheater tube thickness	=	4.5 mm
Exit reheater tube thickness	=	6.0 mm
First extraction steam flow at 90 MW load	=	1.680 Kg/sec.
Second extraction steam flow at 90 MW load	=	1.715 Kg/sec.
Third extraction steam flow at 90 MW load	=	2.616 Kg/sec.
Fourth extraction steam flow at 90 MW load	=	2.82 Kg/sec.
Fifth extraction steam flow at 90 MW load	=	1.86 Kg/sec.
Sixth extraction steam flow at 90 MW load	=	1.358 Kg/sec.
Seventh extraction steam flow at 90 MW load	=	4.97 Kg/sec.
Eighth extraction steam flow at 90 MW load	=	6.38 Kg/sec.
Efficiency of high pressure turbine	=	0.85
Efficiency of medium pressure turbine	=	0.85
Efficiency of low pressure turbine	=	0.80

The following constants are determined for the model at the time of initialisation:

C_0 = 0.0813

C_4 = 0.0649

C_5 = 0.0208

C_6 = 0.0241

C_7 = 0.0465

C_8 = 0.0567

C_{CMW} = 17.1529

C_{HMW1} = 1.8835

C_{HMW2} = 1.2286

C_{HMW3} = 0.99260

C_{HMW4} = 0.80689

C_{HMW5} = 0.64409

C_{HMW6} = 1.2703

C_{RMS1} = 1.4864

C_{RMS2} = 2.7102

F_{R1} = 30.5

F_{R2} = 12.1

K_1 = 0.000055488

K_2 = 0.00965

K_3 = 0.05012

K_4 = 0.040793

K_5 = 0.090966

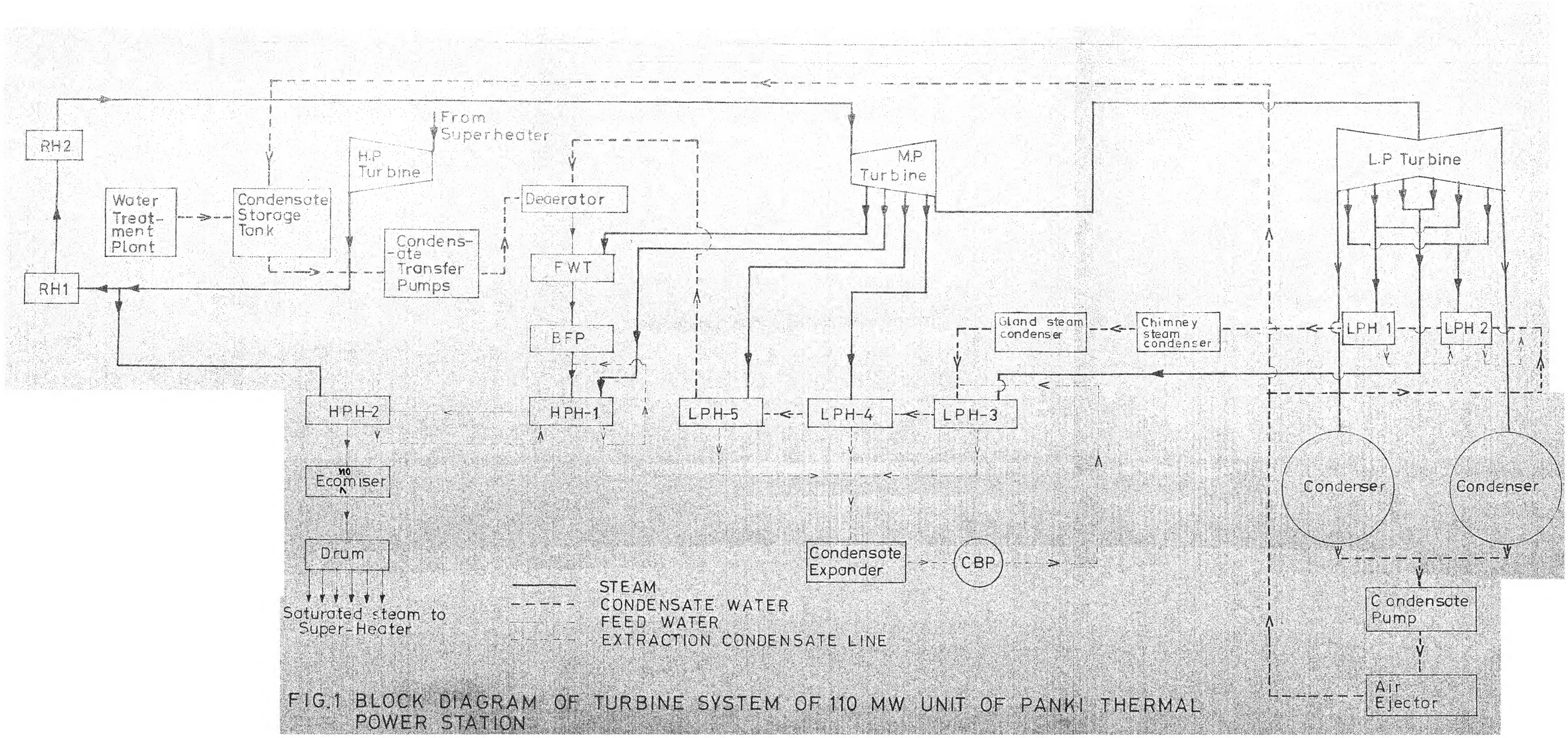

FIG.1 BLOCK DIAGRAM OF TURBINE SYSTEM OF 110 MW UNIT OF PANKI THERMAL POWER STATION

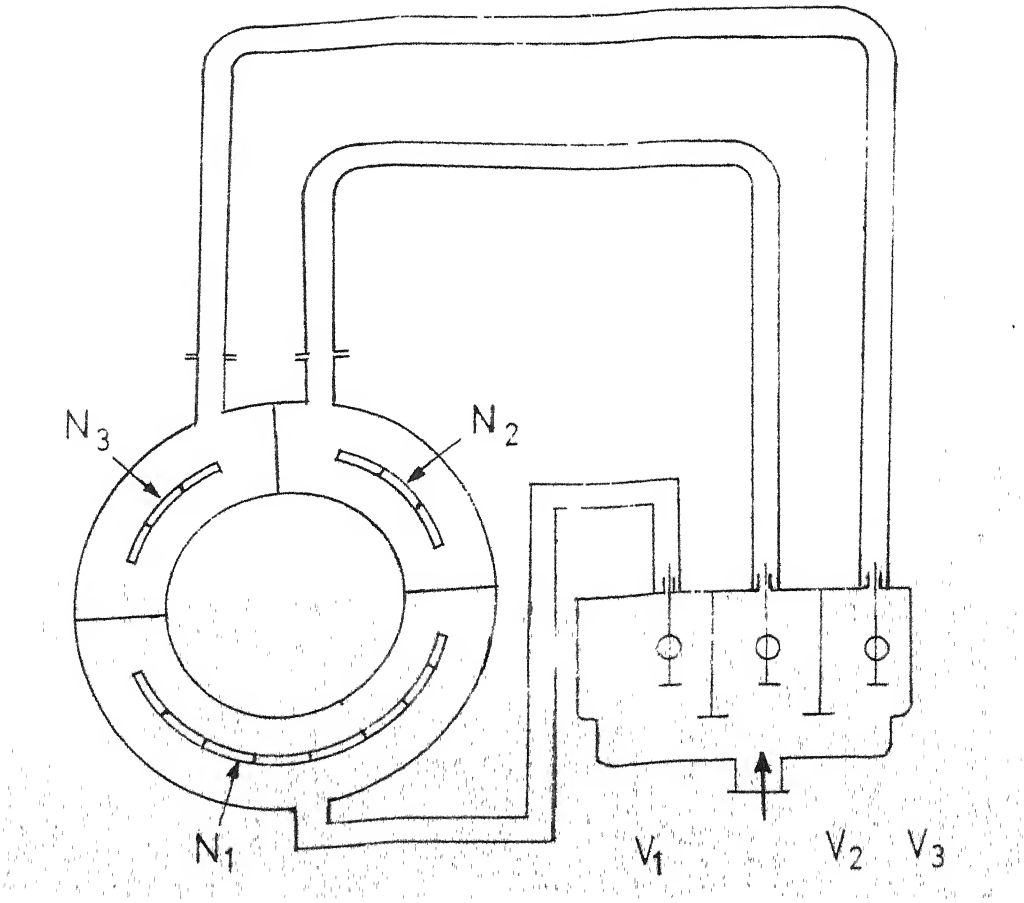

FIG. 2 NOZZLE BOX GOVERNING ARRANGEME

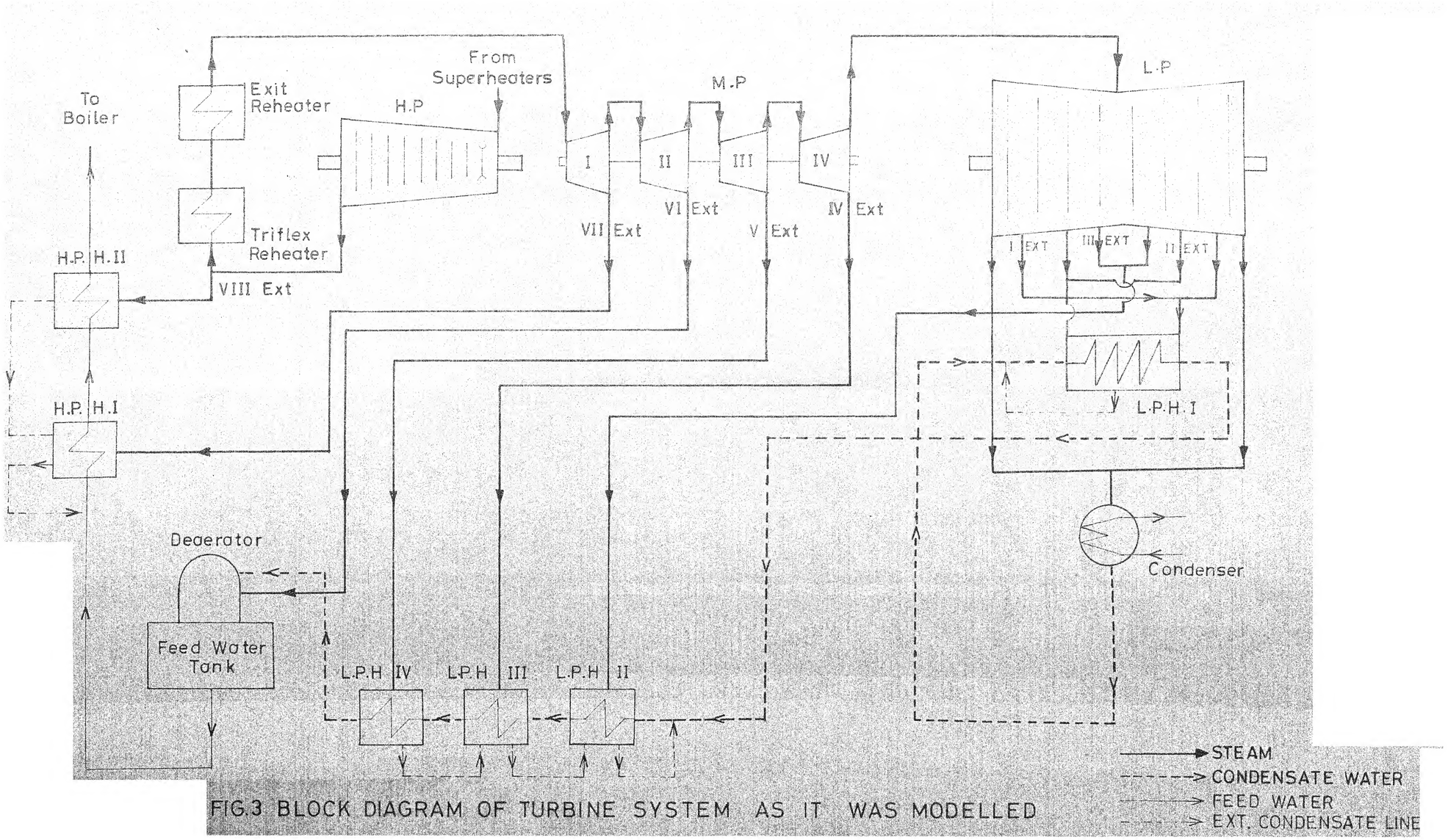

FIG.3 BLOCK DIAGRAM OF TURBINE SYSTEM AS IT WAS MODELLED

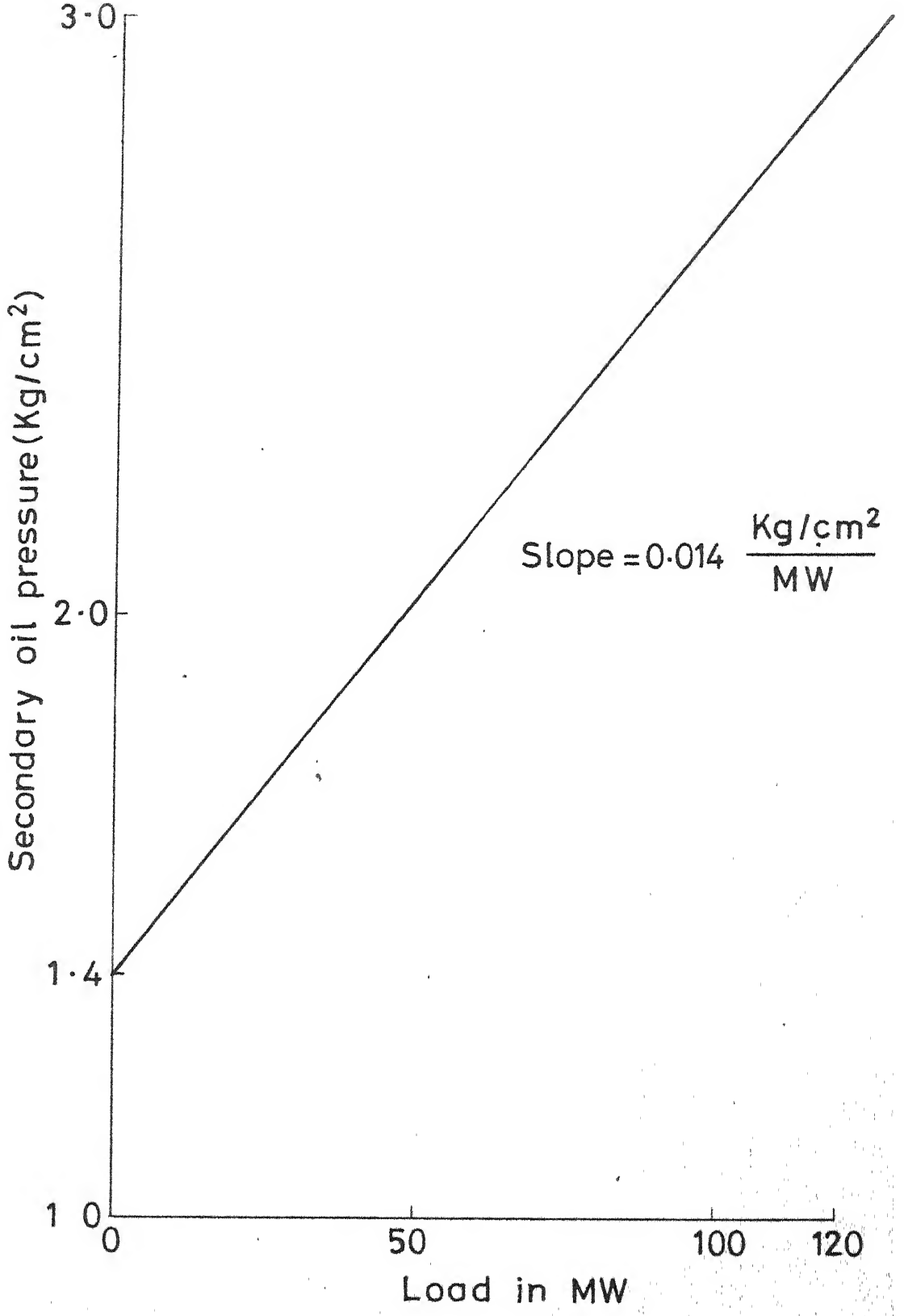

FIG. 5 GRAPH SHOWING OIL PRESSURE V/S LOAD

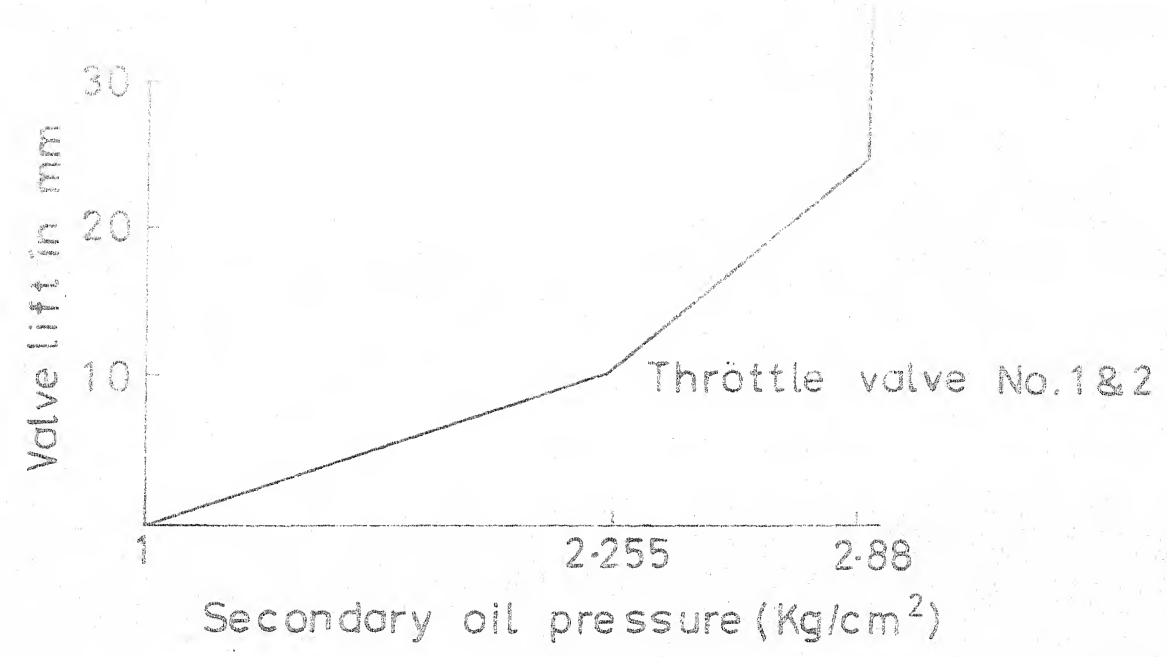

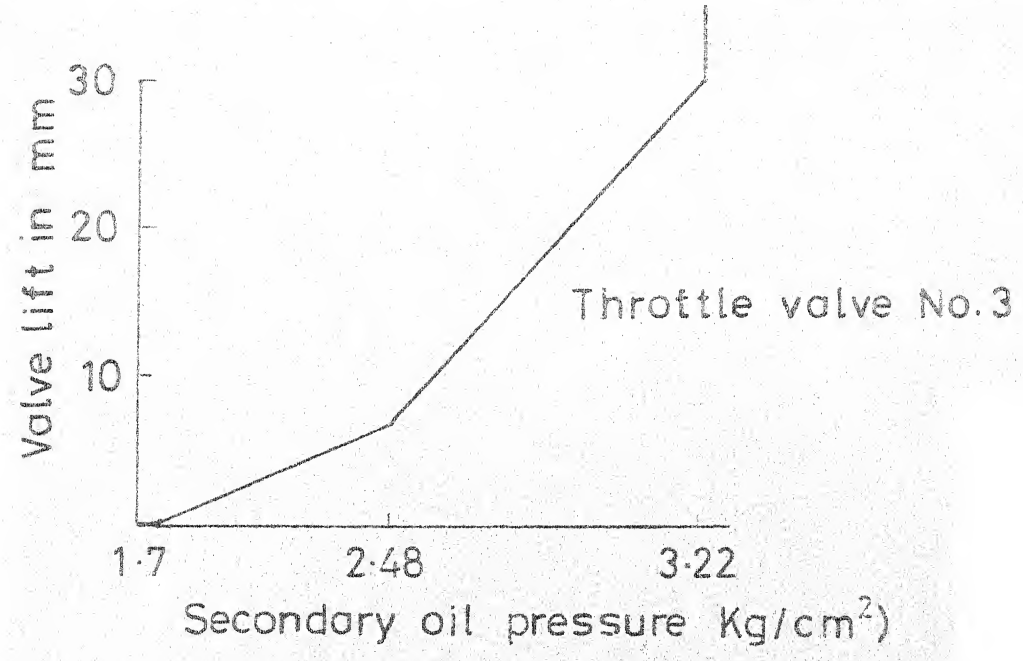

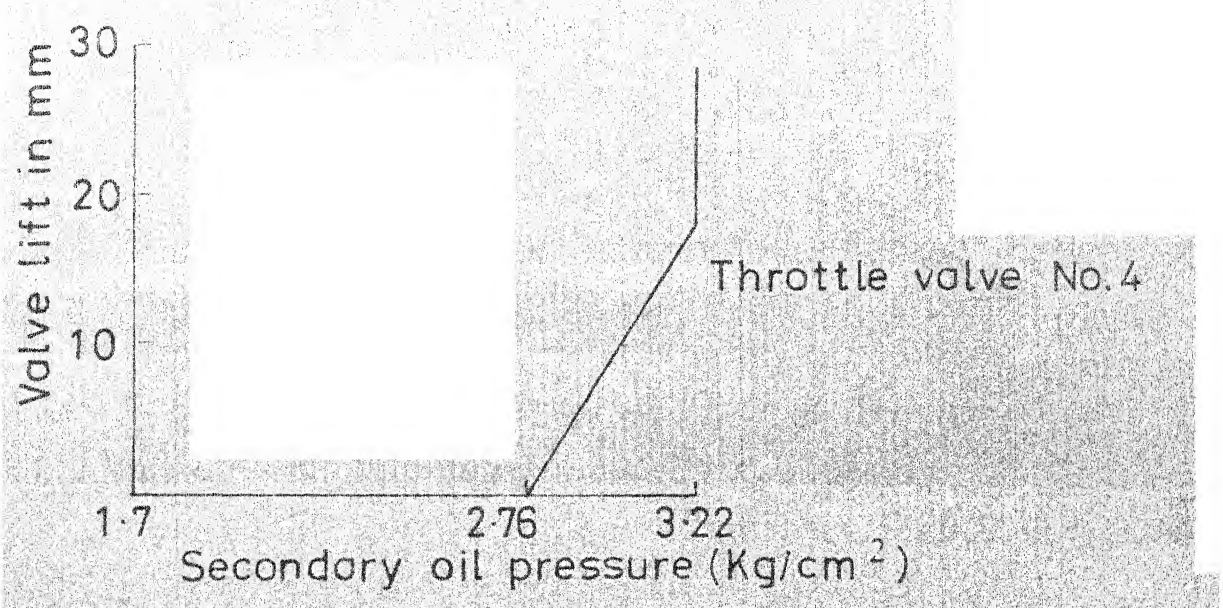

FIG. 6 GRAPHS SHOWING LIFT OF VALVES V/S SECONDARY OIL PRESSURE

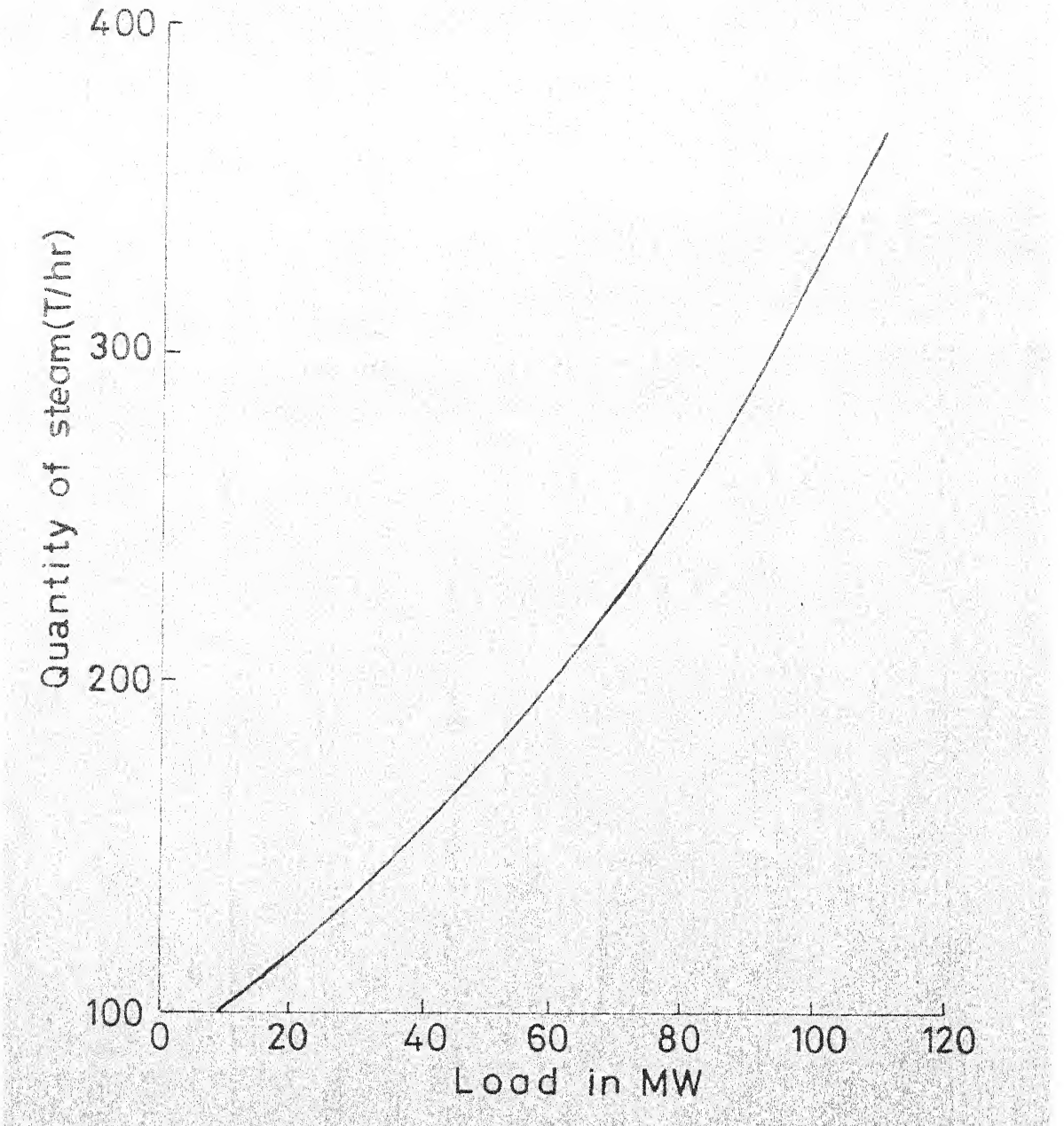

FIG.7 GRAPH SHOWING STEAM FLOW V/S LOAD

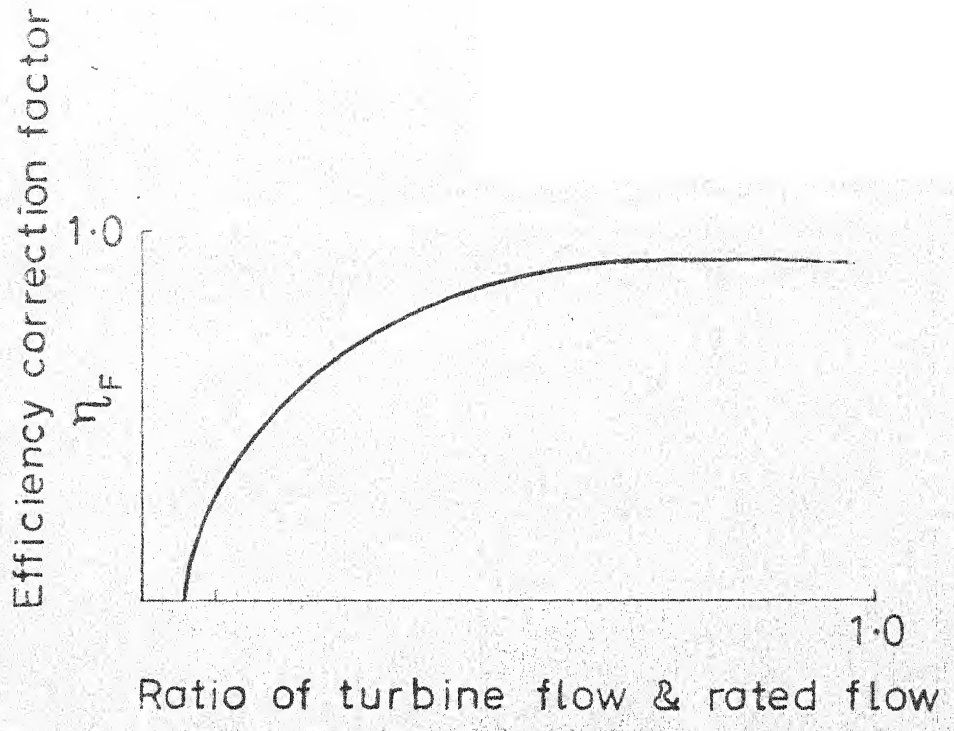

FIG.8 GRAPH SHOWING VARIATION OF EFFICIENCY CORRECTION FACTOR WITH RATIO OF TURBINE FLOW & RATED FLOW

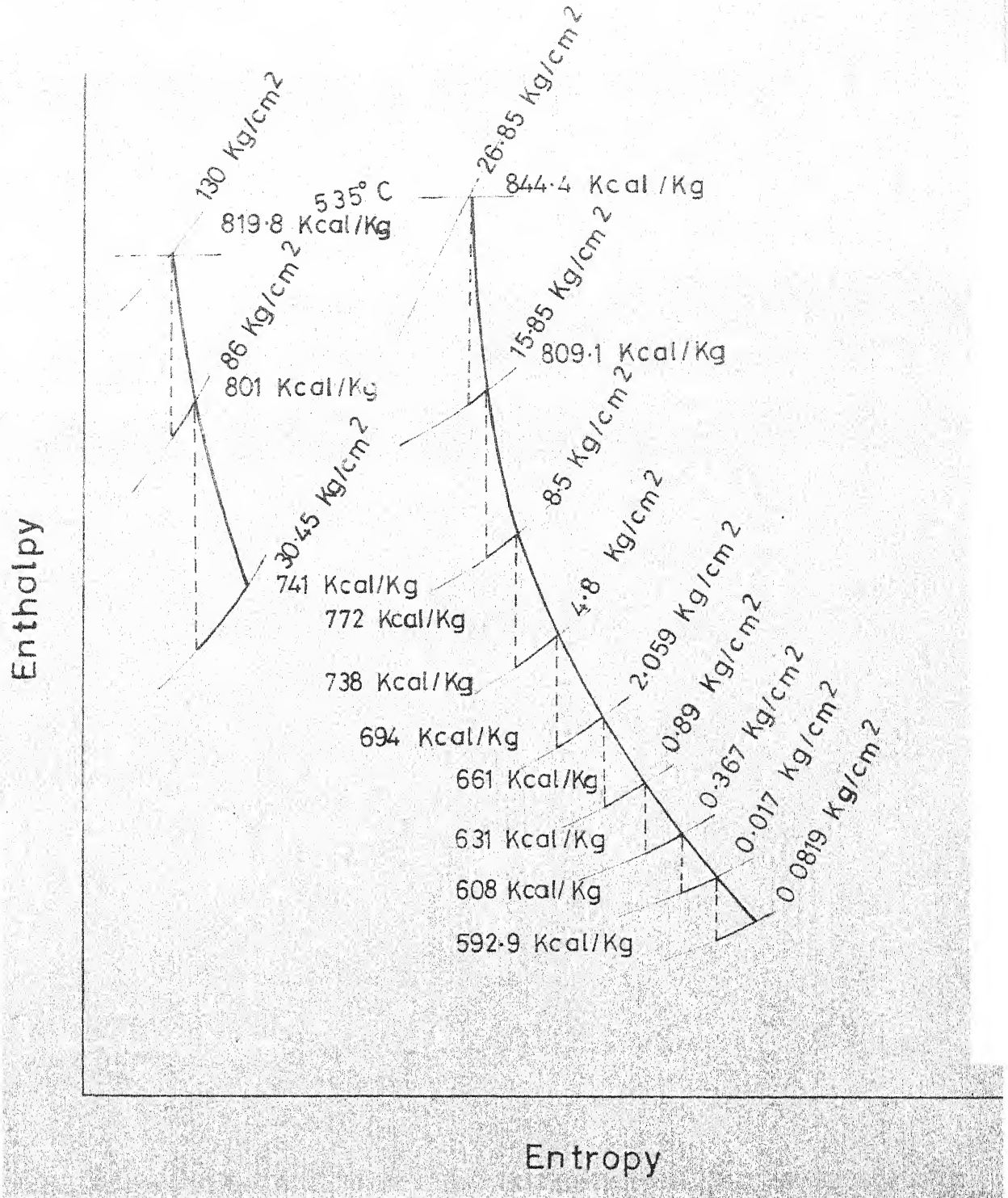

FIG. 9 THERMODYNAMIC REPRESENTATION OF STEAM PATH

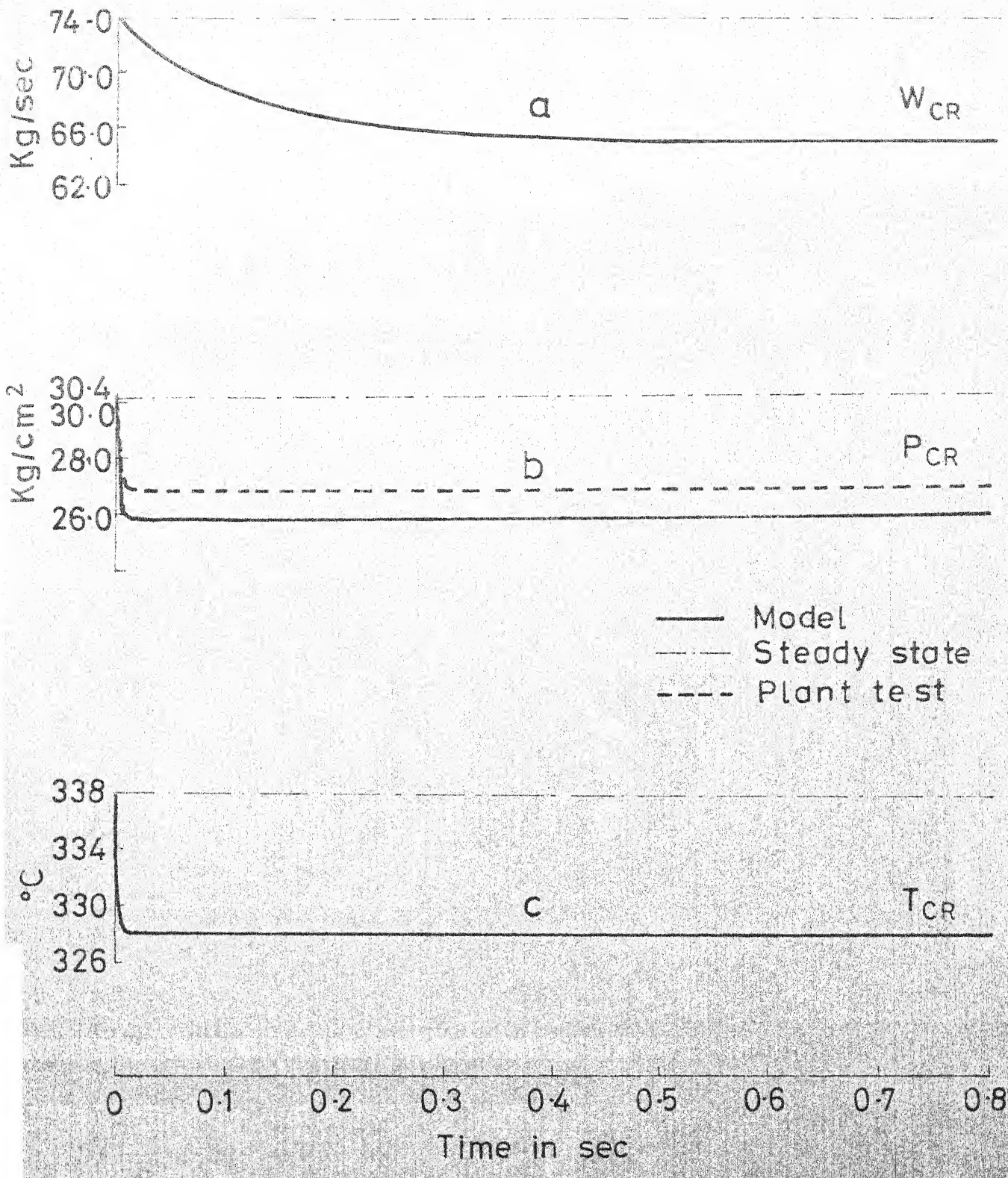

FIG. 10 H.P. TURBINE RESPONSES FOR 10 MW LOAD DROP FROM 90 MW STEADY STATE

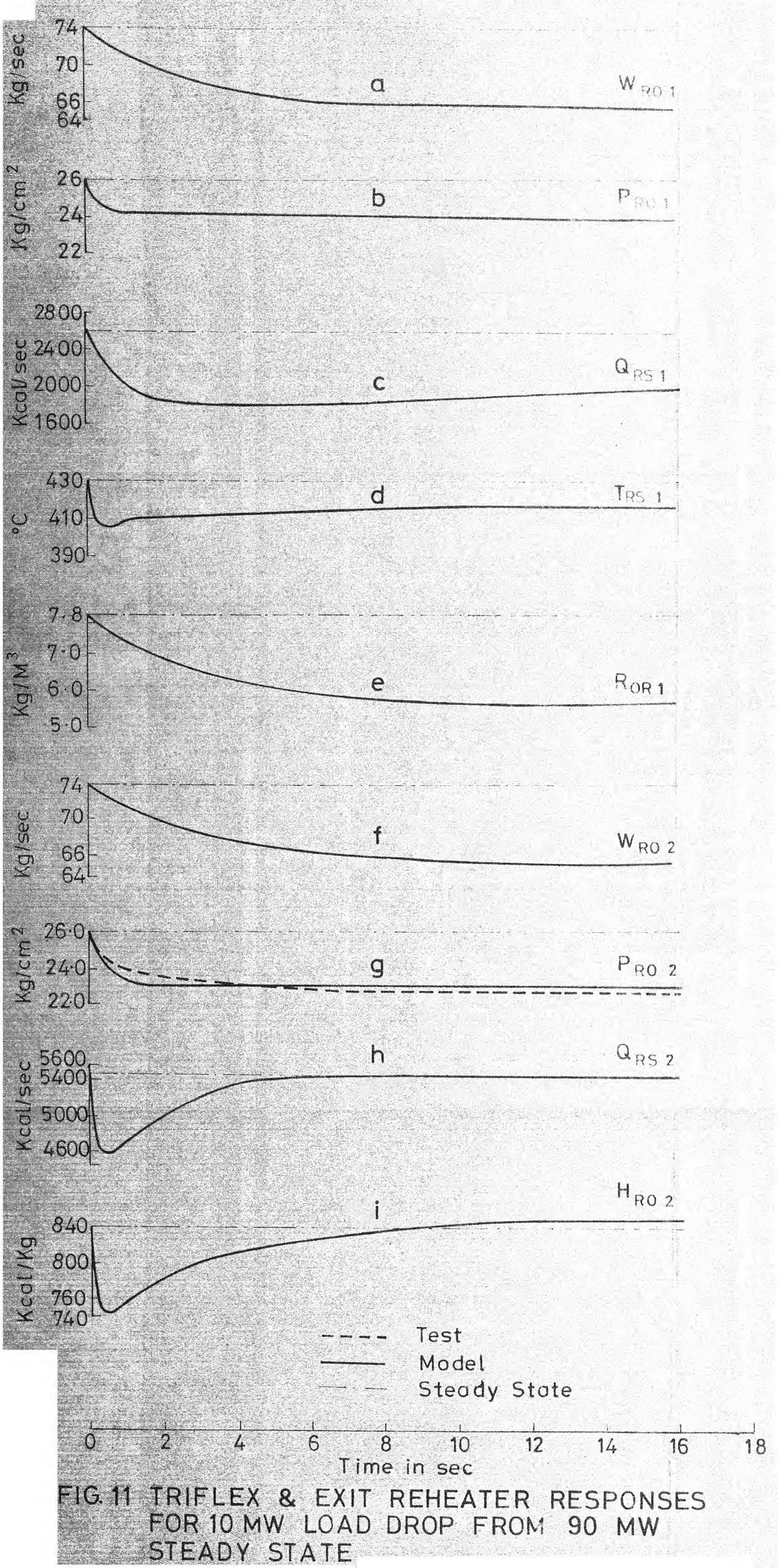

FIG. 11 TRIFLEX & EXIT REHEATER RESPONSES FOR 10 MW LOAD DROP FROM 90 MW STEADY STATE

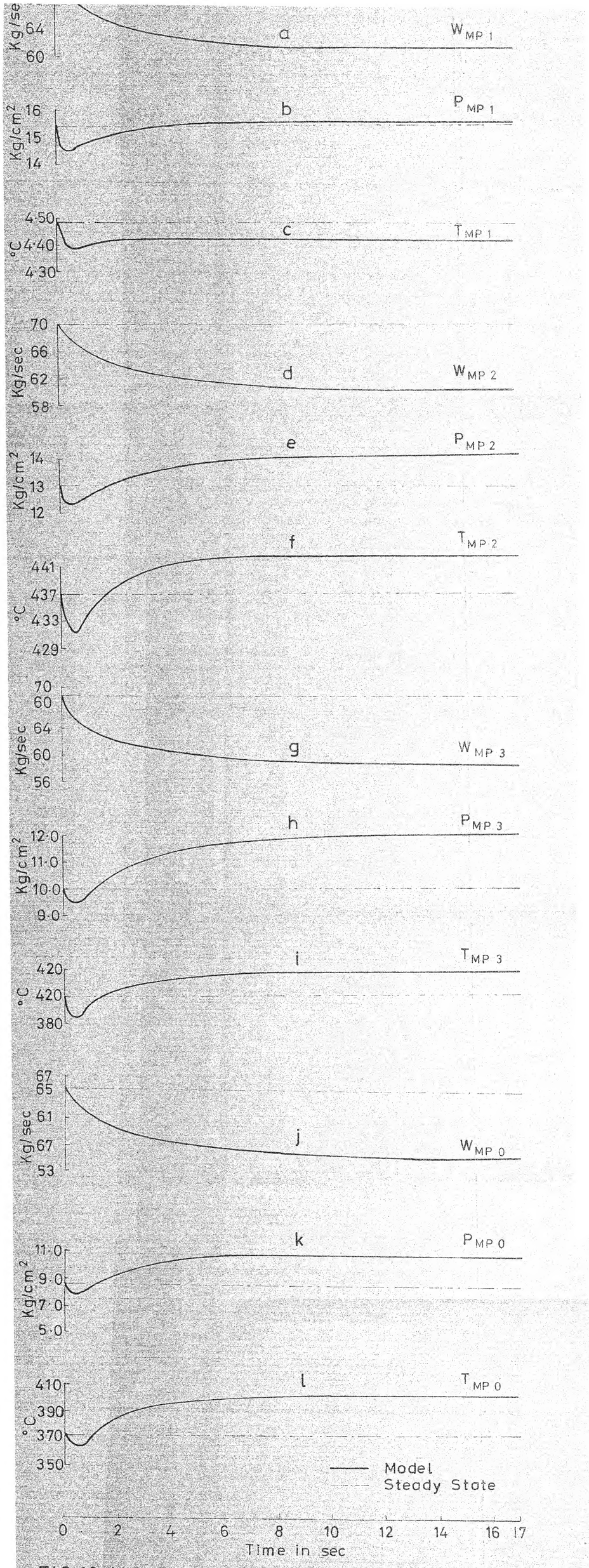

FIG.12 M.P TURBINE RESPONSES FOR 10 MW LOAD DROP FROM 90 MW STEADY STATE

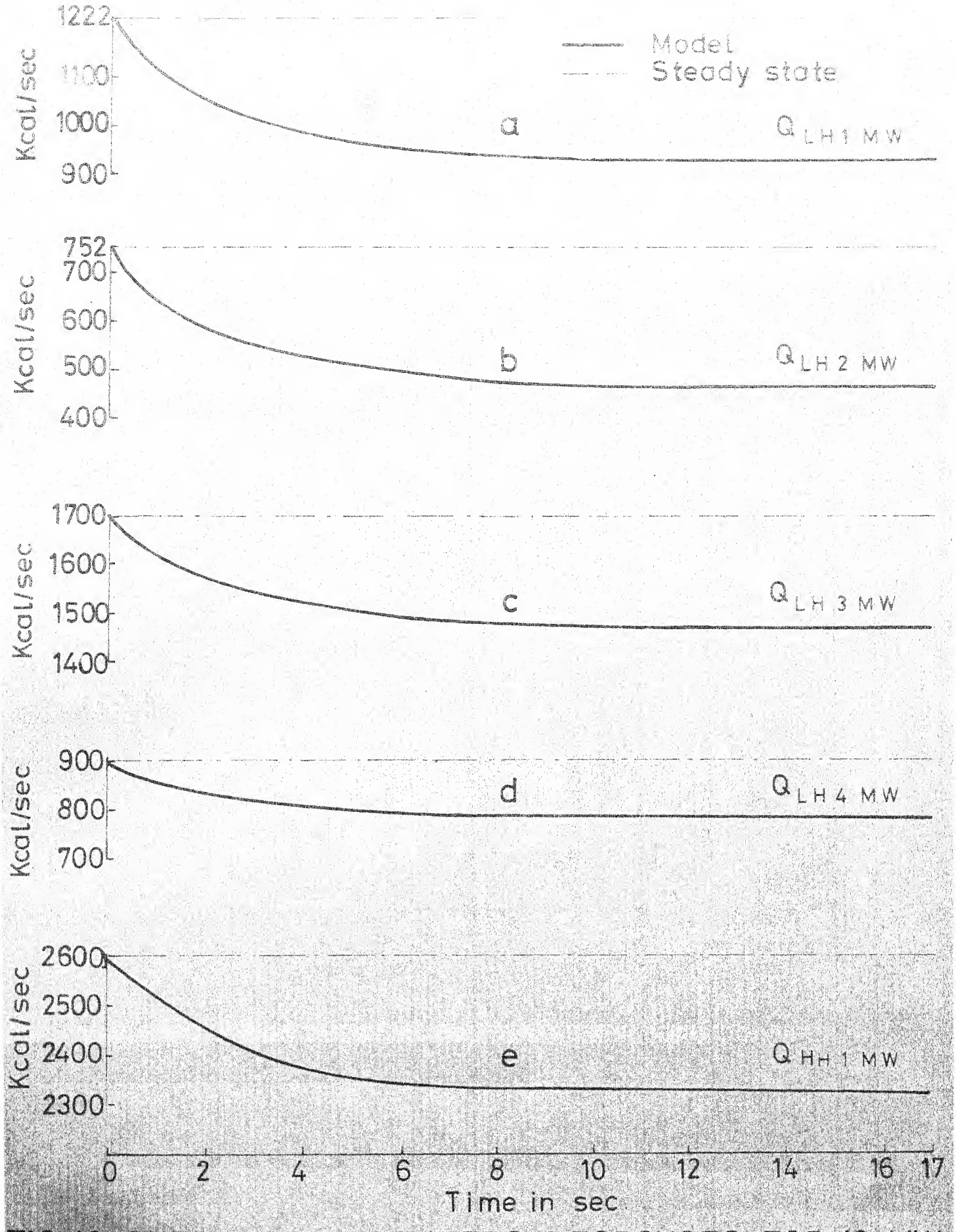

FIG. 13 FEED WATER HEATERS RESPONSES FOR 10 MW LOAD DROP FROM 90 MW STEADY STATE

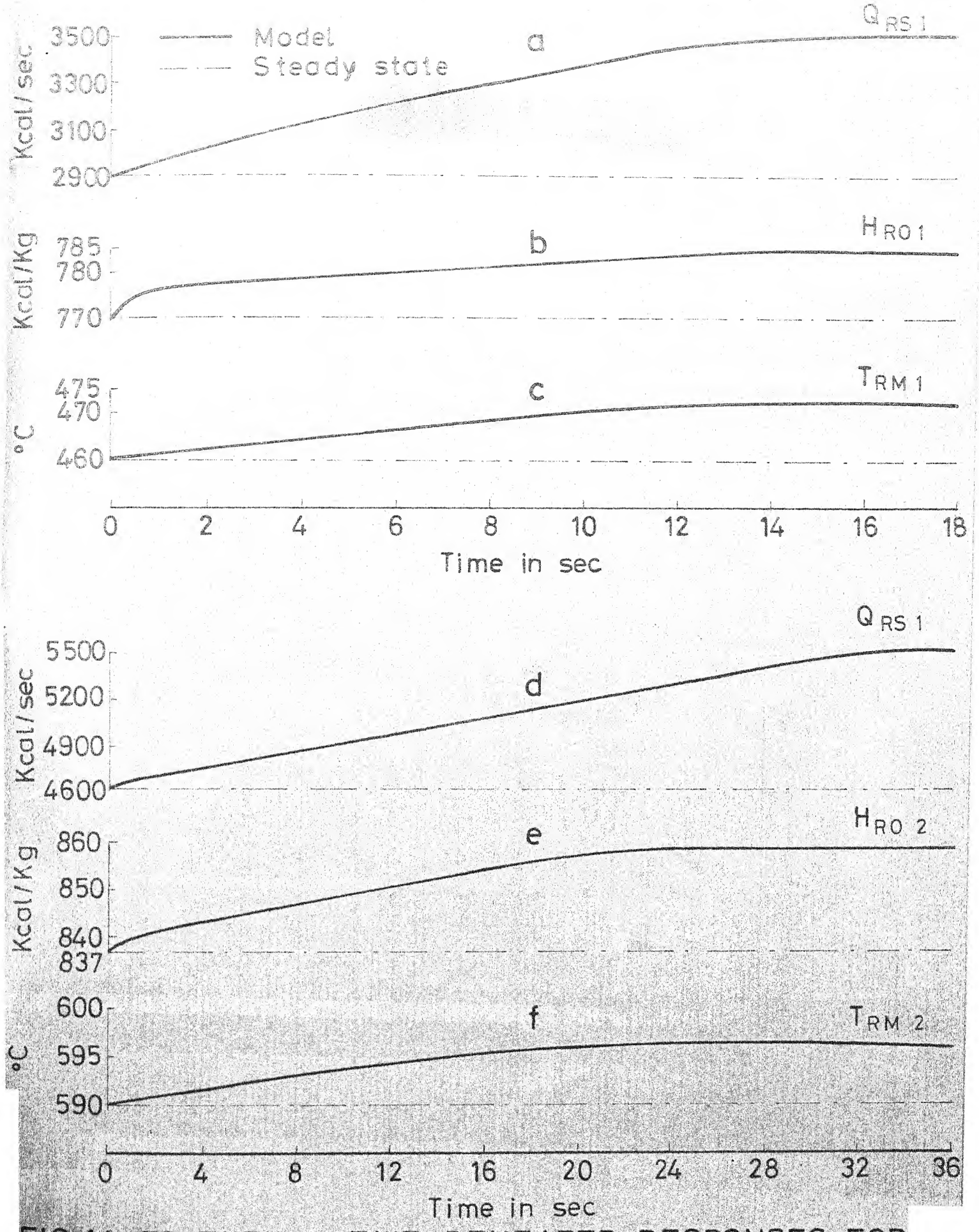

FIG.14 TRIFLEX & EXIT REHEATER RESPONSES FOR A STEP INCREASE IN GAS TO METAL HEAT TRANSFER RATES AT 90 MW STEADY STATE

A 55421

A 55421

Date Slip

This book is to be returned on the date last stamped.

CD 6.72.9

ME-1578-M-SHA-DYN.